Optimal Bit Allocation for CTU Level Rate Control in HEVC

Shengxi Li, *Member, IEEE*, Mai Xu, *Member, IEEE*, Zulin Wang, *Member, IEEE*, and Xiaoyan Sun, *Senior Member, IEEE*

***Abstract*— For High Efficiency Video Coding (HEVC), the R–λ scheme is the latest rate control (RC) scheme, which investigates the relationships among allocated bits, the slope of rate-distortion (R-D) curve λ, and quantization parameter. However, we argue that bit allocation in the existing R–λ scheme is not optimal. In this paper, we therefore propose an optimal bit allocation (OBA) scheme for coding tree unit level RC in HEVC. Specifically, to achieve the OBA, we first develop an optimization formulation with a novel R-D estimation, instead of the existing R–λ estimation. Unfortunately, it is intractable to obtain a closed-form solution to the optimization formulation. We thus propose a recursive Taylor expansion (RTE) method to iteratively solve the formulation. As a result, an approximate closed-form solution can be obtained, thus achieving OBA and bit reallocation. Both theoretical and numerical analyses show the fast convergence speed and little computational time of the proposed RTE method. Therefore, our OBA scheme can be achieved at little encoding complexity cost. Finally, the experimental results validate the effectiveness of our scheme in three aspects: R-D performance, RC accuracy, and robustness over dynamic scene changes.**

***Index Terms*— High Efficiency Video Coding (HEVC), rate control (RC), video coding.**

I. Introduction

A. Background

DUE to the explosive increase of video data over Internet, the bandwidth-hungry issue becomes more and more serious. To overcome such an issue, video coding aims to save bitrates at the cost of video quality loss. Nowadays, with high-definition (HD) and even ultrahigh-definition (UHD) videos being popular, efficient video coding standards are urgently required. H.264/AVC [2], which was finalized in June 2004, cannot meet the demand of huge data produced by HD or UHD videos. Therefore, from 2010, Joint Collaborative Team on Video Coding (JCT-VC) [3] devoted its effort to the next major advance in video coding, i.e., High Efficiency Video Coding (HEVC) [4]. HEVC standard [5] was formally finalized in January 2013 and approved in April 2013, doubling coding efficiency over the preceding H.264/AVC standard [6]. To meet the bandwidth limitation, rate control (RC) has been taken into account for the latest HEVC standard.

In video coding, RC aims at minimizing distortion of compressed videos with constraints on bitrate. Specifically, if the bitrates of compressed videos are larger than the supplied bandwidth, the extra bits will accumulate in the encoder buffer, leading to the loss of some video frames once the buffer overflows. On the contrary, if the bitrates are oversupplied by the bandwidth, the bandwidth may be wasted as more bits can be utilized to improve the compressed video quality. In general, at a given bitrate, RC is achieved by means of optimizing bit allocation and then mapping from allocated bits to quantization parameter (QP). Therefore, the objective of RC schemes in video coding is twofold.

1) *Objective I:* Optimal bit allocation (OBA) to achieve minimal distortion.
2) *Objective II:* Accurate QP estimation to ensure RC accuracy.

B. Related Work

RC has been extensively studied for different video coding standards (TM5 for MPEG-2 [7], VM8 for MPEG-4 [8], and JVT-N046 [9] for H.264). The previous RC schemes can be mainly divided into two categories: Q-domain and ρ-domain schemes. For Q-domain RC schemes, the relationship between bitrate R and QP value, i.e., R–Q relationship, is worked out in [10]–[16]. In most cases, such a relationship is modeled as a quadratic function $R = a+b/Q+c/Q^2$ [10]–[14], [16], where a, b, and c are parameters related to video content. In the work of [14], efficient bit allocation for temporal layers is achieved by integrating a linear quality dependency model with the R–Q and rate-distortion (R-D) models, for scalable video coding in H.264/AVC. Furthermore, besides using quadratic function as the R–Q relationship, Liu *et al.* [13] proposed a novel optimal RC scheme to improve R-D performance of H.264. In their scheme, an optimization formulation is solved to minimize overall distortion at given target bitrates by predicting mean absolute difference (MAD). Recently, to implement both R-D optimization and RC in H.264/AVC, [16] separated the QP used for R-D optimization from that used for quantization, by which the R–Q and distortion-quantization (D-Q) models are correspondingly established. This way, the bitrates can be well controlled, especially for the videos with high and unpredictable scenes. As another way, ρ-domain RC schemes establish the relationship between bitrate R and the percentage of zero-valued transformed coefficients ρ [17]–[19]. However, since HEVC adopts the flexible picture partition,

Manuscript received August 11, 2015; revised January 3, 2016 and March 11, 2016; accepted July 1, 2016. Date of publication July 11, 2016; date of current version November 8, 2017. This work was supported in part by the China 973 Program under Grant 2013CB329006, in part by the National Natural Science Foundation of China Projects under Grant 61573037 and Grant 61471022, and in part by the Fok Ying Tung Education Foundation under Grant 151061. This paper was presented in the IEEE International Conference on Multimedia and Expo 2015 [1]. This paper was recommended by Associate Editor M. Mattavelli. *(Corresponding author: Mai Xu.)*

S. Li and M. Xu are with Beihang University, Beijing 100191, China (e-mail: maixu@buaa.edu.cn).

Z. Wang is with Beihang University, Beijing 100191, China, and also with the Collaborative Innovation Center of Geospatial Technology, Wuhan 430079, China.

X. Sun is with Microsoft Research Asia, Beijing 100080, China.

Color versions of one or more of the figures in this paper are available online at http://ieeexplore.ieee.org.

Digital Object Identifier 10.1109/TCSVT.2016.2589878

parallel coding, and some other cutting-edge technologies, the aforementioned Q-domain and ρ-domain schemes fail to be implemented in HEVC. Therefore, RC schemes need to be redeveloped in HEVC.

Toward *objective II* of RC for HEVC, a pixelwise unified rate quantization scheme [20] has been proposed to allocate bits via introducing a term bpp (i.e., bit per pixel), and to assign QP values using a quadratic equation of target bpp and QP. Such a scheme can be seen as a Q-domain scheme. Further, Si *et al.* [21] proposed an advanced Q-domain scheme by setting up a new R–Q relationship using the sum of absolute transformed difference (SATD). Moreover, a feedback strategy is developed in [21] to avoid sudden increase of QP in poor quality regions, which may result in error propagation for the following frames. For ρ-domain RC schemes, Wang *et al.* [22] established a quadratic ρ-domain rate quantization model for HEVC RC, which utilizes specialized QP determination and reference picture set mechanism. However, according to [23], the R–Q and R–ρ relationships are hard to be precisely estimated, since various flexible coding parameters and structures are applied in HEVC. It thus makes the Q-domain and ρ-domain RC schemes lack in efficiency. Fortunately, Lagrange multiplier λ [24], which stands for the slope of R-D curve, has been investigated. The relationship between λ and bitrate R can be better characterized in comparison with R–Q and R–ρ relationships. In light of the R–λ relationship, a new scheme, namely R–λ scheme, was proposed in [23].

Most recently, there have been many advanced RC schemes that aim to achieve *objective I* of RC in HEVC. In ρ-domain, a new RC scheme [25] was proposed to achieve optimal hierarchical bit allocation at frame level, which relies on a mixed Laplacian distribution, an inter-frame-dependency-based distortion model, and an inter-frame-dependency-based bitrate model. In the λ-domain, the SATD is utilized in [26] and [27] to allocate target bits for the R–λ RC scheme, instead of predicting MAD in [23]. Moreover, Li *et al.* [28] proposed a brief idea of optimization formulation on bit allocation. However, [28] does not realize OBA, since the formulation on OBA is hard to be solved. Instead, the estimated picture λ is empirically set for bit allocation. Some advance works on R–λ relationship can also achieve *objective I* of HEVC RC. For example, in [29], pre-encoding of multiple QPs proceeds to estimate the SATD–R-D relationship for the bit allocation in RC. As for the cost, it largely increases encoding complexity due to the pre-encoding process. Besides, Wang *et al.* [30] proposed a gradient based R–lambda model, which combines gradient per pixel and bpp, to predict frame complexity for intra-frame RC. To improve subjective metric, an advanced R–λ work was proposed in [31] by considering the region of interest for RC of HEVC.

However, most existing advanced RC schemes mainly concentrate on *objective II* for estimating QP with allocated bits, and they do not focus on *objective I* for OBA. To the best of our knowledge, although some advanced works deal with bit allocation for the R–λ scheme (see [28]), there exists no scheme for realizing OBA for RC in HEVC.

C. Our Work and Main Contributions

In this paper, we propose an OBA scheme for coding tree unit (CTU) level RC in HEVC, on the basis of our conference paper [1]. Specifically, through our investigation, we found out that the existing R–λ estimation of [23] is unable to accurately represent R-D relationship. This inaccurate estimation cannot achieve minimal distortion and accurate RC, which are the two ultimate goals of (*objectives I and II*) for RC. Toward these ultimate goals, we first establish a new R-D estimation, instead of R–λ estimation, on updating bitrate, distortion, and λ, such that more accurate relationships among them can be ensured. Based on such estimation, we then develop a formulation on optimizing bit allocation to each CTU. This formulation is able to minimize distortion over the whole video frame at a given bitrate. However, it is impractical to obtain the closed-form solution to our optimization formulation.

Therefore, in our OBA scheme, we propose a new method, recursive Taylor expansion (RTE) method, to obtain the approximate closed-form solution to our formulation via iterating the Taylor expansion. Furthermore, considering the error between actual and target bits, we develop an RTE-based reallocation method to optimally reassign the target bits left for incoming CTUs. As we know, iteration always leads to high burden on computational complexity. We thus analyze the convergence speed of our RTE method from both theoretical and numerical aspects. The analysis shows that the convergence speed is indeed fast, as the approximation error of our formulation decreases to 10^{-10} with no more than three iterations.[1] Note that each iteration only consumes little computational time, as verified by our analysis. In other words, the proposed RTE method can optimize bit allocation with little encoding complexity cost. As a result, combining the more accurate R-D estimation, our OBA scheme is able to optimally allocate bits with little extra complexity cost.

To the best of our knowledge, this paper is the first work to achieve OBA in HEVC with little extra complexity cost. This paper is an extended version of our conference paper [1], with extensive advance works. Specifically, the advances are as follows. First, the R-D estimation is developed with a more precise distortion model for RC in HEVC. Second, an optimal bit reallocation method is proposed to improve RC accuracy while maintaining R-D optimization. Moreover, beyond the numerical analysis, the theoretical analysis is provided to show the computational complexity of the proposed RTE method and OBA scheme. The code of our OBA scheme is available online: *https://github.com/ShengxiLi/oba_scheme*. The main contributions of this paper are listed below.

1) We develop a new optimization formulation for bit allocation with the proposed R-D estimation. This R-D estimation, as a foundation of our OBA scheme, contributes to both *objectives I and II* in RC of HEVC.
2) We propose a new method, namely, RTE method, for providing an approximate closed-form solution to the optimization formulation. As a result, the OBA and

[1]For each iteration, only a few arithmetic operations are required.

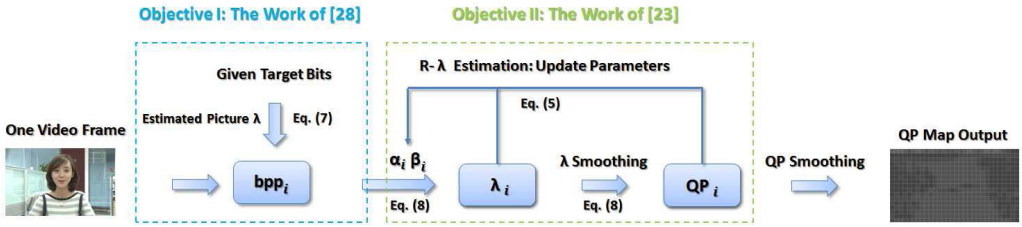

Fig. 1. Procedure of the existing R–λ RC scheme.

reallocation can be accomplished for RC in HEVC. Moreover, theoretical and numerical analyses show that little extra time is required by our scheme.

II. Review on the R–λ Scheme

In this section, we review the existing RC scheme [23], [28] of HEVC, which estimates the R–λ relationship for bit allocation. The main objective of RC is allocating bits to each coding part via rate-distortion optimization. As such, distortion of the compressed video can be minimized at a given bitrate. Since our scheme mainly works at CTU level, we only focus on reviewing CTU level RC. The existing R–λ RC scheme is the combination of [23] and [28]. Specifically, the R–λ scheme can be divided into two stages. First, toward *objective I*, target bits are allocated to each CTU using the estimated picture λ [28]. Second, toward *objective II*, once target bits are allocated, the related parameters can be calculated for yielding QPs based on the R–λ estimation [23]. The main steps of the existing R–λ RC scheme are illustrated in Fig. 1 and discussed below.

The goal of bit allocation within a video frame is to minimize overall distortion D at a given total amount of target bits R, formulated by

$$\min_{\{r_i\}_{i=1}^{M}} \quad D = \sum_{i=1}^{M} d_i \quad \text{s.t.} \quad \sum_{i=1}^{M} r_i \le R \tag{1}$$

where d_i and r_i are the distortion and target bits for the ith CTU. M is the total number of CTUs in the frame. Given Lagrange multiplier λ, (1) can be converted to an unconstrained optimization problem [24]

$$\min_{\{r_i\}_{i=1}^{M}} \sum_{i=1}^{M} (d_i + \lambda r_i). \tag{2}$$

Next, (2) can be solved via setting its derivative to zero

$$\lambda = -\frac{\partial d_i}{\partial r_i} \quad \text{and} \quad \sum_{i=1}^{M} r_i = R, \quad i = 1, 2 \ldots M. \tag{3}$$

In (3), there are $M + 1$ equations with $M + 1$ unknown variables: λ and $\{r_i\}_{i=1}^{M}$. Consequently, (3) can be uniquely solved.

For solving (3), there are many models [24], [32]–[34] to work out the relationship between d_i and r_i by R-D curve fitting. However, as HEVC adopts many new features on video coding, Li *et al.* [23] found that the hyperbolic model [32], [33] performs better than other models. Such a model can be expressed by $d_i = c_i r_i^{-k_i}$, where $c_i(>0)$ and $k_i(>0)$ are fitting parameters related to the content of the ith CTU [23]. Based on the hyperbolic model, the R–λ estimation can be acquired

$$\lambda = -\frac{\partial d_i}{\partial r_i} = c_i k_i \cdot (\text{bpp}_i \cdot N_i)^{-k_i - 1} = \alpha_i \cdot \text{bpp}_i^{\beta_i}. \tag{4}$$

In (4), there exists $r_i = \text{bpp}_i \cdot N_i$ for each CTU, where N_i and bpp_i are the number of pixels and target bpp related to the ith CTU. Moreover, $\alpha_i = c_i k_i \cdot (N_i)^{-k_i - 1}$ and $\beta_i = -k_i - 1$ are the parameters for estimating the R–λ relationship (i.e., the relationship between bpp_i and λ). In practice, α_i and β_i are unknown and may be different from one CTU to another. So, they need to be estimated for the subsequent frames after encoding each CTU, according to its actual consumed bpp_i (denoted by $\text{bpp}_{a,i}$) and actual λ_i (denoted by $\lambda_{a,i}$) [23]. However, the R–λ relationship cannot be accurately estimated when updating α_i and β_i, since there are two variables (α_i and β_i) to be solved in a single equation of (4). In [23], δ_α and δ_β are introduced to estimate α_i and β_i during updating

$$\begin{aligned} \alpha_i' &= \alpha_i + \delta_\alpha \cdot \left(\ln \lambda_{a,i} - \ln\left(\alpha_i \text{bpp}_{a,i}^{\beta_i}\right)\right) \cdot \alpha_i \\ \beta_i' &= \beta_i + \delta_\beta \cdot \left(\ln \lambda_{a,i} - \ln\left(\alpha_i \text{bpp}_{a,i}^{\beta_i}\right)\right) \cdot \ln \text{bpp}_{a,i}. \end{aligned} \tag{5}$$

In (5), α_i' and β_i' represent the updated α_i and β_i for the ith CTU; δ_α and δ_β are parameters reflecting the updating speed. As can be seen from (5), since δ_α and δ_β are empirically set, the R–λ and R-D relationships cannot be accurately estimated by α_i and β_i along with the scene changes. Such an inaccurate estimation may make the RC scheme hard to achieve *objectives I and II* in HEVC. Therefore, we propose to estimate R-D relationship in Section III-A as the foundation of our OBA scheme.

Based on the R–λ estimation of (4) and (5), (3) can be rewritten in the following form for bit allocation:

$$\sum_{i=1}^{M} r_i = \sum_{i=1}^{M} (\text{bpp}_i \cdot N_i) = \sum_{i=1}^{M} \left(\left(\frac{\lambda}{\alpha_i} \right)^{1/\beta_i} \cdot N_i \right) = R. \tag{6}$$

Unfortunately, since α_i and β_i are generally different among CTUs, it is intractable to acquire the closed-form solution for λ in (6). An approximate way [28] is to apply the estimated picture λ (denoted by λ_p) in (6), which is calculated at the frame level [23]. Then, the following equations can be

used [28] to allocate target bits:

$$\begin{cases} \text{bpp}_i = \dfrac{r_i}{N_i} \\ r_i = R \cdot \eta_i \Big/ \displaystyle\sum_{j=1}^{M} \eta_j \\ \eta_i = \left(\dfrac{\lambda_p}{\alpha_i}\right)^{\left(\frac{1}{\beta_i}\right)}. \end{cases} \tag{7}$$

In (7), η_i stands for the weight of the ith CTU. Recall that R is the target bit for the whole frame.

However, since λ_p is not a closed-form solution to (6), there exists $\sum_{i=1}^{M} \eta_i \cdot N_i \neq R$. To satisfy the bitrate constraint, the bitrates are adjusted by $\eta_i / \sum_{j=1}^{M} \eta_j$ in (7). However, the bitrate adjustment largely degrades the R-D performance. It is because $r_i = R \cdot \eta_i / \sum_{j=1}^{M} \eta_j$ does not satisfy $\lambda = -(\partial d_i / \partial r_i)$ in (3), so distortion minimization of (1) cannot be achieved. Therefore, we propose an RTE method to solve (6) with an approximate closed-form solution. This way, the R-D performance can be improved while satisfying the bitrate constraint. Our RTE method is to be introduced in Section IV.

At last, as illustrated in Fig. 1, once bpp_i is allocated for each CTU by (7), RC can be achieved via estimating its corresponding λ_i and QP_i

$$\begin{aligned} \lambda_i &= \alpha_i \cdot \text{bpp}_i^{\beta_i} \\ \text{QP}_i &= 4.2005 \cdot \ln\lambda_i + 13.7122. \end{aligned} \tag{8}$$

For more details about estimation of λ_i and QP_i, refer to [23].

In summary, the bit allocation of the existing R–λ RC scheme, which is the combination of [23] and [28], is not an optimal one due to the following two issues.

1) The solution of α_i and β_i in (5) is inaccurate for solving (4) in [23]. This issue is to be addressed in Section III.
2) Equation (7) is an empirical solution to (4) in [28], which is far from the closed-form solution. This issue is to be addressed in Section IV.

III. Proposed R-D Estimation

As we have argued in Section II, the R–λ estimation is unable to optimally allocate bits to each CTU and precisely estimate QP. To overcome the above disadvantages, in Section III-A we propose to estimate R-D relationship, instead of R–λ relationship, as the foundation of our OBA scheme. In addition, the R-D estimation enjoys the advantage of reducing the gap between the target and actual bits, compared with the R–λ estimation. Finally, to validate the effectiveness of our R-D estimation, numerical analysis is provided in Section III-B.

A. R-D Estimation for the Proposed OBA Scheme

Since the ultimate goal of RC is to minimize distortion d_i at a given bitrate bpp_i, it is more reasonable to estimate the relationship between d_i and bpp_i (i.e., R-D relationship), instead of λ_i and bpp_i. Fortunately, after encoding each CTU, the actual d_i can also be obtained, such that one more equation is available to estimate the R-D relationship. Therefore, we propose to use the R-D estimation for our OBA scheme, which can be achieved by the updating of c_i and k_i as follows.

Combining the hyperbolic model $d_i = c_i r_i^{-k_i}$ and (4), the following equations hold after encoding the ith CTU:

$$\begin{aligned} d_{a,i} &= c_i r_{a,i}^{-k_i} \\ \lambda_{a,i} &= c_i k_i r_{a,i}^{-k_i - 1}. \end{aligned} \tag{9}$$

Here, $\lambda_{a,i}$, $r_{a,i}$, and $d_{a,i}$ are the actual λ value, bits, and distortion for the ith CTU. Note that there are two variables (c_i and k_i) to be estimated with the above two equations. It means that after encoding the ith CTU, c_i and k_i can be uniquely solved by

$$c_i = \frac{d_{a,i}}{r_{a,i}^{-\lambda_{a,i} \cdot r_{a,i} / d_{a,i}}} \quad \text{and} \quad k_i = \frac{\lambda_{a,i} \cdot r_{a,i}}{d_{a,i}} \tag{10}$$

for encoding the collocated CTUs in the following frames. Note that for each CTU, c_i and k_i can be updated without any empirical setting. Thus, our R-D estimation can be achieved by (10) with known parameters $\lambda_{a,i}$, $r_{a,i}$, and $d_{a,i}$ for the ith CTU. Since the updating of c_i and k_i is straightforward in (10) to solve (9) rather than the gradual updating in (5), our R-D estimation can well reflect the content of each CTU, enhancing RC accuracy for *objective II*. Furthermore, based on the straightforward updating of c_i and k_i, the OBA of our OBA scheme can be achieved (to be discussed in Section IV), thus achieving *objective I* of RC.

B. Analysis of the R–λ and R-D Estimations

For validating the accuracy of our R-D estimation, we have analyzed all 16 JCT-VC standard test video sequences [35] with the R–λ [23] and R-D estimations. In our test, the videos were compressed by HM 14.0, with the configuration being the same as that given in Section VI-A. Note that both hierarchical and nonhierarchical RC were tested, with the bitrates being the same as QP = 37, 32, 27, and 22. More details about parameter settings are given in Section VI-A.

For comparison, we use the absolute difference between the estimated and actual distortion for each CTU as the metric. It is defined as

$$E_{d,i} = \left| \frac{d_{e,i} - d_{a,i}}{d_{a,i}} \right| \tag{11}$$

where $d_{e,i}$ denotes the estimated distortion of the ith CTU. It is calculated by the actual bpp (i.e., bpp_i) and its corresponding estimation (i.e., R–λ or R-D estimation). Recall that $d_{a,i}$ denotes the actual distortion for the ith CTU. In our analysis, the distortion is evaluated by mean square error (MSE).

Since the relationship between bpp_i and d_i can be directly represented by c_i and k_i for our R-D estimation, the estimated distortion is calculated by

$$d_{e,i} = c_i \text{bpp}_{a,i}^{-k_i}. \tag{12}$$

However, for the R–λ estimation, since α_i and β_i estimate the relationship between λ and bpp_i, we need to convert them to c_i and k_i when calculating $E_{d,i}$ using (11). In [23], there

TABLE I

COMPARISON OF DISTORTION ESTIMATION ACCURACY BETWEEN THE R–λ [23] AND R-D ESTIMATIONS OVER ALL 16 VIDEO SEQUENCES AT HIERARCHICAL (H) AND NONHIERARCHICAL (NH) SETTINGS

		416 × 240				832 × 480				1080 × 720			1920 × 1080				
		RaceHorse	*BlowingBubbles*	*BasketballPass*	*BQSquare*	*BasketballDrill*	*PartyScene*	*RaceHorseC*	*BQMall*	*Johnny*	*KristenAndSara*	*Fourpeople*	*BasketballDrive*	*Kimono*	*BQTerrace*	*ParkScene*	*Cactus*
NH	[23]	9.89	9.86	12.06	4.15	11.48	2.80	7.45	9.62	16.71	26.40	17.47	10.08	15.65	4.79	9.02	5.87
	Our	0.11	0.12	0.17	0.75	0.15	0.76	1.74	0.51	0.24	0.12	0.24	0.14	0.80	0.33	0.26	0.18
H	[23]	4.46	5.69	6.02	3.68	16.37	5.74	6.28	9.06	18.63	17.83	12.18	9.49	11.94	3.50	8.54	5.35
	Our	0.35	0.09	0.77	0.07	7.35	0.20	2.58	4.15	0.73	0.17	0.64	0.10	8.07	1.00	1.45	0.40

exist $\alpha_i = c_i k_i \cdot (N_i)^{-k_i-1}$ and $\beta_i = -k_i - 1$, as presented in (4). Thus, for the R–λ estimation, $d_{e,i}$ can be calculated by

$$d_{e,i} = \frac{\alpha_i}{(-\beta_i - 1) \cdot N_i^{\beta_i}} \cdot \mathrm{bpp}_{a,i}^{\beta_i+1}. \tag{13}$$

Finally, $E_{d,i}$ for each CTU can be obtained by (11) for both our R-D and R–λ estimations.

Table I reports the results of averaged $E_{d,i}$ of all CTUs by our R-D and R–λ [23] estimations when compressing each video sequence at four bitrates. It can be seen from this table that for the R–λ scheme, the gap between the estimated and actual distortion is extremely large, which causes $E_{d,i} \gg 1$. This indicates the inaccurate R–λ estimation of distortion. Furthermore, we can see that our R-D estimation is significantly better than the R–λ estimation, as $E_{d,i} < 1$ for most video sequences. Therefore, this validates the improvement of the proposed R-D estimation in the accuracy of distortion estimation.

IV. APPROXIMATE CLOSED-FORM SOLUTION FOR THE OBA SCHEME

This section focuses on the OBA scheme for CTU level RC in HEVC. Specifically, Section IV-A develops the OBA formulation upon (6) with our R-D estimation. Unfortunately, it is intractable to obtain the closed-form solution to this formulation. Thus, Section IV-B utilizes Taylor expansion to solve this formulation. Nevertheless, the Taylor expansion solution may cause a large approximation error, resulting in nonoptimal bit allocation. Instead, Section IV-C proposes the RTE method, which iterates Taylor expansion to obtain an approximate closed-form solution to optimal CTU bit allocation. At last, Section IV-D proposes to optimally reallocate the remaining target bits after encoding each CTU based on our RTE method. Such a reallocation is capable of reducing the deviation between the target and actual bits of each CTU. This way, both *objectives I* and *II* can be achieved.

A. Optimization Formulation for Bit Allocation

Based on the R-D estimation of c_i and k_i, we rewrite the optimization formulation of (6) on CTU bit allocation as follows:

$$\sum_{i=1}^{M} r_i = \sum_{i=1}^{M} \left(\frac{\lambda}{c_i k_i}\right)^{-\frac{1}{k_i+1}} = \sum_{i=1}^{M} \left(\frac{a_i}{\lambda}\right)^{b_i} = R \tag{14}$$

where $a_i = c_i k_i$ and $b_i = (1/k_i + 1)$. However, since b_i varies among CTUs, it is hard to derive a closed-form solution to λ. Thus, we propose a new method, the RTE method, to solve (14) for obtaining the OBA with little complexity cost. Before presenting our RTE method, the Taylor expansion solution is discussed as the basis.

B. Taylor Expansion Solution

To deal with different exponents b_i in (14), we rewrite $(a_i/\lambda)^{b_i}$ by utilizing Taylor expansion

$$\left(\frac{a_i}{\lambda}\right)^{b_i} = 1 + \frac{\ln\left(\frac{a_i}{\lambda}\right)}{1!} b_i + \cdots + \frac{\left(\ln\frac{a_i}{\lambda}\right)^n}{n!} b_i^n + \cdots \tag{15}$$

Then, we discard the biquadratic and higher order terms in the Taylor expansion. As a result, the following approximation holds:

$$\begin{aligned}\left(\frac{a_i}{\lambda}\right)^{b_i} &\approx 1 + \frac{\ln\left(\frac{a_i}{\lambda}\right)}{1!} b_i + \frac{\left(\ln\frac{a_i}{\lambda}\right)^2}{2!} b_i^2 + \frac{\left(\ln\frac{a_i}{\lambda}\right)^3}{3!} b_i^3 \\ &= -\frac{b_i^3}{6}\ln^3\lambda + \left(\frac{b_i^2}{2} + \frac{b_i^3}{2}\ln a_i\right)\ln^2\lambda \\ &\quad -\left(b_i^2 \ln a_i + b_i + \frac{b_i^3}{2}\ln^2 a_i\right)\ln\lambda \\ &\quad + \left(1 + b_i \ln a_i + \frac{b_i^2}{2}\ln^2 a_i + \frac{b_i^3}{6}\ln^3 a_i\right).\end{aligned} \tag{16}$$

Accordingly, (14) can be approximated by

$$\begin{aligned} R &= \sum_{i=1}^{M} \left(\frac{a_i}{\lambda}\right)^{b_i} \\ &\approx \underbrace{-\sum_{i=1}^{M}\left(\frac{b_i^3}{6}\right)}_{A}\ln^3\lambda + \underbrace{\sum_{i=1}^{M}\left(\frac{b_i^2}{2} + \frac{b_i^3}{2}\ln a_i\right)}_{B}\ln^2\lambda \\ &\quad \underbrace{-\sum_{i=1}^{M}\left(b_i^2\ln a_i + b_i + \frac{b_i^3}{2}\ln^2 a_i\right)}_{C}\ln\lambda \\ &\quad + \underbrace{\sum_{i=1}^{M}\left(1 + b_i\ln a_i + \frac{b_i^2}{2}\ln^2 a_i + \frac{b_i^3}{6}\ln^3 a_i\right)}_{D}. \end{aligned} \tag{17}$$

Applying Shengjin formula [36], the cubic equation in (17) is worked out to obtain the estimated λ (denoted by $\hat{\lambda}$). Note that as $\Delta = F^2 - 4EG > 0$ in practical encoding, there exists only one real solution for (17). Therefore, $\hat{\lambda}$ value is unique for OBA. When further discarding the cubic order term, (17) becomes a quadratic equation. We found that such a quadratic equation may have no real solution, so the OBA via solving (17) cannot be achieved. Even when the quadratic equation has real solutions, it is usually with two real solutions, such that our RTE method (to be discussed in Section IV-C) is hard to be implemented. Therefore, instead of discarding the cubic and higher order terms, the biquadratic and high-order terms of Taylor expansion are removed from (17) for our OBA scheme. Then, $\hat{\lambda}$ can be obtained as follows:

$$\begin{aligned} \widehat{\lambda} &= e^{\frac{-B-(\sqrt[3]{Y_1}+\sqrt[3]{Y_2})}{3A}} \\ Y_{1,2} &= BE + 3A\left(\frac{-F \pm \sqrt{F^2-4EG}}{2}\right) \end{aligned} \tag{18}$$

where $E = B^2 - 3AC$, $F = BC - 9A(D-R)$, and $G = C^2 - 3B(D-R)$. At last, given $\hat{\lambda}$, the bit allocation can be achieved using (14).

However, since the value of $\ln(a_i/\lambda)$ is normally very large in practical encoding, the truncation of higher order terms in Taylor expansion may result in great approximation error in (17). As a result, $\hat{\lambda}$ obtained by (18) is not the best, so the bit allocation is not sufficiently optimal. Therefore, the RTE method is proposed to recursively implement Taylor expansion for reducing the approximation error.

C. Recursive Taylor Expansion Solution

As discussed above, the truncation of higher order terms in (15) may result in a large approximation error when applying Taylor expansion in Section IV-B. In fact, the approximation error depends on the decay rate of Taylor expansion, and large decay rate leads to small approximation error. Here, the decay rate is defined as

$$\left|\frac{\frac{\left(\ln\frac{a_i}{\lambda}\right)^n}{n!}{b_i}^n}{\frac{\left(\ln\frac{a_i}{\lambda}\right)^{n+1}}{(n+1)!}{b_i}^{n+1}}\right| = \left|\frac{n+1}{\left(\ln\frac{a_i}{\lambda}\right)\cdot b_i}\right|. \tag{19}$$

As seen from (19), it is possible to increase the decay rate of Taylor expansion by reducing the value of $|\ln a_i/\lambda|$ (i.e., $(a_i/\lambda) \to 1$). To this end, we replace $(a_i/\lambda)^{b_i}$ by $\tilde{r}_i(\tilde{\lambda}/\lambda)^{b_i}$ via decomposing a_i, where $\tilde{\lambda}$ ($(\tilde{\lambda}/\lambda) \to 1$) is the pre-estimated λ of the currently compressed frame, and $\tilde{r}_i = (a_i/\tilde{\lambda})^{b_i}$ is the pre-estimated target bit for the ith CTU. Then, (14) can be rewritten as

$$\sum_{i=1}^{M}\left(\frac{a_i}{\lambda}\right)^{b_i} = \sum_{i=1}^{M}\tilde{r}_i\left(\frac{\tilde{\lambda}}{\lambda}\right)^{b_i} = R. \tag{20}$$

Similar to (16), the following approximation on $(a_i/\lambda)^{b_i}$ holds:

$$\begin{aligned} \left(\frac{a_i}{\lambda}\right)^{b_i} &= \tilde{r}_i\left(\frac{\tilde{\lambda}}{\lambda}\right)^{b_i} \\ &= \tilde{r}_i + \tilde{r}_i\frac{\ln\left(\frac{\tilde{\lambda}}{\lambda}\right)}{1!}b_i + \tilde{r}_i\frac{\left(\ln\frac{\tilde{\lambda}}{\lambda}\right)^2}{2!}b_i^2 + \cdots + \tilde{r}_i\frac{\left(\ln\frac{\tilde{\lambda}}{\lambda}\right)^n}{n!}b_i^n + \cdots \\ &\approx \tilde{r}_i\left(1 + \frac{\ln\left(\frac{\tilde{\lambda}}{\lambda}\right)}{1!}b_i + \frac{\left(\ln\frac{\tilde{\lambda}}{\lambda}\right)^2}{2!}b_i^2 + \frac{\left(\ln\frac{\tilde{\lambda}}{\lambda}\right)^3}{3!}b_i^3\right). \end{aligned} \tag{21}$$

According to (19), the decay rate of Taylor expansion in (21) is $|(n+1/(\ln(\tilde{\lambda}/\lambda))\cdot b_i)|$, which is much larger than the decay rate in (15) when $|\ln(\tilde{\lambda}/\lambda)| \ll |\ln(a_i/\lambda)|$ and $b_i > 0$. Consequently, the approximation error of Taylor expansion can be reduced, as proved in Lemma 1.

Lemma 1: Provided that $|(n+1/\ln(a_i/\lambda)b_i)| < |(n+1/\ln(\tilde{\lambda}/\lambda)b_i)|$ and $(a_i/\lambda)^{b_i} = \tilde{r}_i(\tilde{\lambda}/\lambda)^{b_i}$, the following inequality holds:

$$\begin{aligned} &\left|\left(\frac{a_i}{\lambda}\right)^{b_i} - 1 - \frac{\ln\left(\frac{a_i}{\lambda}\right)}{1!}b_i - \frac{\left(\ln\frac{a_i}{\lambda}\right)^2}{2!}b_i^2 - \cdots - \frac{\left(\ln\frac{a_i}{\lambda}\right)^N}{N!}b_i^N\right| \\ &> \left|\tilde{r}_i\left(\frac{\tilde{\lambda}}{\lambda}\right)^{b_i} - \tilde{r}_i - \tilde{r}_i\frac{\ln\left(\frac{\tilde{\lambda}}{\lambda}\right)}{1!}b_i \right. \\ &\quad \left. - \tilde{r}_i\frac{\left(\ln\frac{\tilde{\lambda}}{\lambda}\right)^2}{2!}b_i^2 - \cdots - \tilde{r}_i\frac{\left(\ln\frac{\tilde{\lambda}}{\lambda}\right)^N}{N!}b_i^N\right| \end{aligned} \tag{22}$$

where $a_i > \lambda > 0$, $\tilde{\lambda} > \lambda > 0$, $b_i > 0$, and $R > 0$.

Proof: See Appendix A.

As seen from Lemma 1, the approximation error of (21) is less than that of (17), when $|\ln(\tilde{\lambda}/\lambda)| < |\ln(a_i/\lambda)|$. Consider a special case that $\tilde{\lambda} = \lambda$. In this case, there exists no approximation error of (21), as $\ln(\tilde{\lambda}/\lambda) = 0$ makes the decay rate approach infinity. Accordingly, $\tilde{r}_i$ is the OBA for each CTU.

Therefore, based on the third-order Taylor approximation of (21), (20) can be rewritten as

$$\begin{aligned} R = \sum_{i=1}^{M}\tilde{r}_i\left(\frac{\tilde{\lambda}}{\lambda}\right)^{b_i} &\approx \underbrace{-\sum_{i=1}^{M}\left(\tilde{r}_i\frac{b_i^3}{6}\right)}_{A'}\ln^3\lambda \\ &+ \underbrace{\sum_{i=1}^{M}\tilde{r}_i\left(\frac{b_i^2}{2} + \frac{b_i^3}{2}\ln\tilde{\lambda}\right)}_{B'}\ln^2\lambda \\ &\underbrace{-\sum_{i=1}^{M}\tilde{r}_i\left(b_i^2\ln\tilde{\lambda} + b_i + \frac{b_i^3}{2}\ln^2\tilde{\lambda}\right)}_{C'}\ln\lambda \\ &+ \underbrace{\sum_{i=1}^{M}\tilde{r}_i\left(1 + b_i\ln\tilde{\lambda} + \frac{b_i^2}{2}\ln^2\tilde{\lambda} + \frac{b_i^3}{6}\ln^3\tilde{\lambda}\right)}_{D'}. \end{aligned} \tag{23}$$

Finally, $\hat{\lambda}$, as the estimated solution of λ to (23), can be obtained with A, B, C, and D replaced by A', B', C', and D' in (18). Note that $\hat{\lambda}$ acquired from (23) is with less approximation error than that from (17).

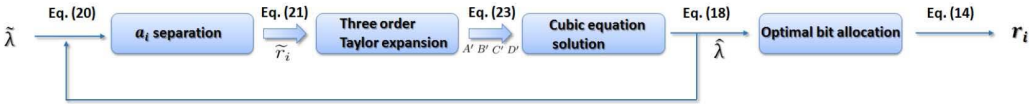

Fig. 2. Overall procedure of the RTE method.

Next, it is possible to further reduce the approximation error of (23) by making $\tilde{\lambda}$ close to the best λ. However, it is impossible to obtain the best λ in practical encoding, as the best λ is a variable to be solved. Thus, there is a chicken-and-egg dilemma between $\tilde{\lambda}$ and the best λ. In fact, we can iterate the Taylor expansion by utilizing the estimated solution $\hat{\lambda}$ as the input $\tilde{\lambda}$ to the next iteration. Then, the approximation error can be reduced alongside the iterations once Lemma 2 exists. Note that Lemma 2 requires $0 < \tilde{\lambda} < \lambda$. If $\tilde{\lambda} > \lambda > 0$ at the first iteration, its output $\hat{\lambda}$ is smaller than λ, as pointed out by Proposition 1. Then, for the subsequent iterations, $0 < \tilde{\lambda} < \lambda$ can be achieved, since the value of $\tilde{\lambda}$ has been replaced by that of $\hat{\lambda}$.

Proposition 1: Consider $\tilde{\lambda} > 0$, $\lambda > 0$, $b_i > 0$, $\lambda \neq \tilde{\lambda}$, and $R > 0$ for (23). If $\hat{\lambda}$ is the solution of λ to (23), then the following holds:

$$\hat{\lambda} < \lambda. \tag{24}$$

Proof: See Appendix B.

Lemma 2: Consider $\lambda > \tilde{\lambda} > 0$, $b_i > 0$, and $R > 0$ for (23). When the solution of λ to (23) is $\hat{\lambda}$, the following inequality holds for $\hat{\lambda}$:

$$|\hat{\lambda} - \lambda| < |\tilde{\lambda} - \lambda|. \tag{25}$$

Proof: See Appendix C.

With iterations, our RTE method can be achieved, which is summarized in Fig. 2. To be more specific, the RTE method is composed of the following steps.

1) *Step 1:* Initialize pre-estimated $\tilde{\lambda}$ to be the picture λ.
2) *Step 2:* Calculate A', B', C', and D' of (23) with $\tilde{\lambda}$.
3) *Step 3:* Obtain $\hat{\lambda}$ by solving (18).
4) *Step 4:* Update $\tilde{\lambda}$ by $\hat{\lambda}$ obtained from step 3, for the next iteration.
5) *Step 5:* Judge whether $\hat{\lambda}$ meets the convergence criterion. If satisfying the convergence criterion, go to step 6. Otherwise, go to step 2.
6) *Step 6:* Apply $\widehat{r}_i = (a_i/\hat{\lambda})^{b_i}$ with the above-obtained $\hat{\lambda}$, where $\widehat{r}_i$ is the OBA to each CTU.

Note that in practice, the picture λ is closer to the best λ than a_i. For initialization, we set the initial $\tilde{\lambda}$ as the picture λ [23], which has been calculated for the RC at frame level. For iteration, the convergence criterion is set to be $|\sum_{i=1}^{M} \widehat{r}_i - R|/R < 10^{-10}$. Normally, our RTE method is able to converge to 10^{-10} approximation error, with no more than three iterations. After three or less iterations, RTE can reduce the difference between $\hat{\lambda}$ and the best λ to an extremely small range, meeting the convergence criterion. Thus, $\hat{\lambda}$ can be seen as the approximate closed-form solution to the best λ of (14). As such, the bits can be optimally allocated to each CTU. More details about the convergence analysis of our RTE method is presented in Section V.

D. RTE-Based Bit Reallocation Method

In practical HEVC encoding, the actually consumed bits in each CTU may be different from the target bits assigned to this CTU. Therefore, the target bits for the incoming CTUs should be adjusted. In the R–λ RC scheme [23], the error between actual and target bits is compensated by averaging it into the next several CTUs to be encoded. Such a process is called bit reallocation. However, this reallocation method suffers from nonoptimization when reassigning the target bits. For more details, refer to [23].

In this section, we develop a more reasonable bit reallocation method, benefiting from the OBA of our RTE method. More specifically, for compensating the bitrate error after encoding the ith CTU, the target bits for the incoming K CTUs (denoted by $T_{i+1,i+K}$) are reallocated by

$$T_{i+1,i+K} = \sum_{j=i+1}^{j=i+K} \widehat{r}_j + \underbrace{\left(\widehat{T} - \sum_{j=i+1}^{j=M} \widehat{r}_j\right)}_{\text{bit}-\text{rate error}}. \tag{26}$$

In (26), $\widehat{T}$ is the left bit for encoding remaining CTUs in the current frame. Recall that M means the total number of CTUs in the frame, and $\widehat{r}_j$ represents the optimally preallocated target bits for the jth CTU by our RTE method in Section IV-C. Apparently, as seen from (26), the bitrate error is to be compensated after encoding the next K CTUs. Here, the RTE method of Section IV-C is applied to optimally reallocate $T_{i+1,i+K}$ to the next K CTUs. Note that we follow [23] to set $K = 4$, which means that bits are reassigned in the next four CTUs. Moreover, it needs to be pointed out that due to the fast convergence of our RTE method, the complexity increases little when implementing our optimal bit reallocation.

In summary, when encoding a video frame, we first use the RTE method to optimally preallocate the target bits of the currently encoding frame. Then, to reduce the gap between the actual and target bits for each CTU, our RTE-based bit reallocation is applied to optimally reassign target bits to the incoming CTUs. As a result, our OBA scheme is able to advance the state-of-the-art RC of HEVC due to the OBA and reallocation.

V. Complexity Analysis Over the OBA Scheme

For HEVC, the computational complexity is crucial. It is thus necessary to analyze the computational complexity of our OBA scheme. Since the RTE method is the core of our OBA scheme, we first analyze the convergence speed of the RTE method from both theoretical and numerical perspectives. Then, the computational time for one frame of our OBA scheme is provided, verifying the little extra computational complexity cost of our OBA scheme.

A. Theoretical Analysis

For theoretical analysis, we here investigate the difference between $\hat{\lambda}$ and λ alongside the iterations of our RTE method. Recall that $\hat{\lambda}$ is the estimated solution of λ to (14), and λ means the best λ of (14). Thus, the difference between $\hat{\lambda}$ and λ reflects the convergence of our RTE method, and it can be defined by

$$\left|\frac{\hat{\lambda}-\lambda}{\lambda}\right|. \tag{27}$$

If $|\hat{\lambda}-\lambda/\lambda| \rightarrow 0$, it indicates that our RTE method is convergent. As such, we take into consideration the variation of $|\hat{\lambda}-\lambda/\lambda|$ along with each iteration in order to analyze the convergence speed of our RTE method.

In practice, $k_i > 0$ of (14) varies in a small range when encoding each video by HEVC. Therefore, we assume that b_i $(0 < b_i = (1/k_i + 1) < 1)$ remains constant for simplicity. Based on this assumption, the convergence speed of our RTE method to solve (14) can be estimated by Lemma 3.

Lemma 3: Consider that $\tilde{\lambda} > 0$, $\hat{\lambda} > 0$, $\lambda > 0$, $R > 0$, and $\forall i$, $b_i = l \in (0, 1)$. Recall that $\tilde{\lambda}$ is the estimated λ of (20) before each iteration and that $\hat{\lambda}$ is the estimated solution of λ to (14) after each iteration. Equation (14) is the equivalent form of (20). Then, $|((\hat{\lambda}-\lambda)/\lambda/(\tilde{\lambda}-\lambda)/\lambda)|$ decreases at a magnitude of 10^{-3} after each iteration of our RTE method.

Proof: See Appendix D.

According to Lemma 3, $|(\hat{\lambda}-\lambda)/\lambda| < 10^{-3} \cdot |(\tilde{\lambda}-\lambda)/\lambda|$ holds for each iteration of our RTE method. It thus ensures that $|(\hat{\lambda}-\lambda/\lambda)|$ is extremely small after three iterations, quickly approaching 0. As a result, our OBA scheme is able to obtain the approximate closed-form solution with a fast convergence speed.

B. Numerical Analysis

Now, we move to the numerical analysis of the convergence speed of our RTE method. As discussed above, our RTE method owns a fast convergence speed, as $|\hat{\lambda}-\lambda/\lambda|$ quickly approaches 0. However, the best λ of (14) cannot be obtained in practical encoding. Fortunately, since the solution $\hat{\lambda}$ to (14) is unique, $|\sum_{i=1}^{M}(a_i/\hat{\lambda})^{b_i} - R|/\sum_{i=1}^{M}(a_i/\hat{\lambda})^{b_i}$ implies the same convergence performance as $|\hat{\lambda}-\lambda/\lambda|$. We thus define

$$E_a = \frac{\left|\sum_{i=1}^{M}\left(\frac{a_i}{\hat{\lambda}}\right)^{b_i} - R\right|}{\sum_{i=1}^{M}\left(\frac{a_i}{\hat{\lambda}}\right)^{b_i}} \tag{28}$$

as the approximation error of our RTE method. Once $E_a = 0$, $\hat{\lambda}$ is the exactly accurate solution to (14), i.e., the best λ.

In Fig. 3, we plot E_a versus iterations of our RTE method. From this figure, we can see that E_a decreases to below 10^{-10} with no more than three iterations. This is also in accordance with the theoretical analysis above, implying the fast convergence speed of our RTE method.

C. Computational Complexity

Finally, the computational complexity of our OBA scheme is discussed in this section. As analyzed above, the RTE method, which is the core of our OBA scheme, is able to converge within three iterations. In the following, the computational time for one iteration of the proposed RTE method is first estimated. Then, based on such estimated computational time, the computational complexity for our OBA scheme is analyzed.

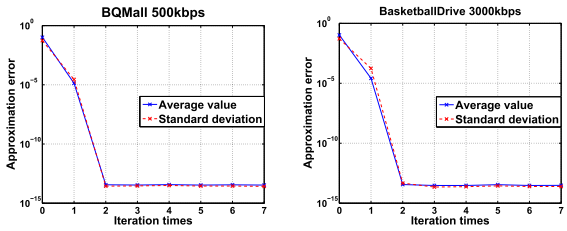

Fig. 3. Average values and standard deviations of approximation error E_a for each iteration of our RTE method. Note that the results of two randomly selected video sequences are provided, and similar results can be found in other sequences.

As mentioned in Section IV-C, the computational complexity of the RTE method is independent of the video contents during bit allocation and reallocation. Thus, we have recorded the computational time for one iteration of our RTE method on a randomly selected video sequence. The computer used for the test is with Intel Core i7-4770 CPU at 3.4 GHz and 16 GB RAM. Through the test, we found out that one iteration of our RTE method only consumes around 0.0015 ms for each CTU. Since it takes at most three iterations to acquire the approximate closed-form solution, the computational time for each solution is up to 0.0045 ms.

Our OBA scheme consists of two parts: bit allocation and bit reallocation. For bit allocation, the OBA scheme only requires three iterations, thus costing up to 0.0045 ms for one frame. For bit reallocation, the OBA scheme takes at most 2.3 ms for all 510 CTUs of each 1080p video frame, since each CTU consumes at most 0.0045 ms for three iterations of our RTE method. For a video frame, 2.3 ms consumed by our OBA scheme is negligible, in comparison with the encoding time of HM 14.0. We further found from the experimental results that less than 0.01‰ extra encoding time is required when introducing the OBA scheme for RC in HM 14.0. Even for real-time encoding, the total computational time of our OBA scheme for one frame is much less than 16.67 ms (the requirement of real-time encoding on 1080p @60 Hz videos). Note that in practical encoding, one or two iterations for most CTUs are enough to obtain the approximate closed-form solution. Thus, the computational time of our scheme for each frame is even much less than 2.3 ms.[2] This implies that our scheme is practicable in real-time encoding. In summary, our OBA scheme has an extremely low approximation error for all CTUs, with little extra computational complexity cost.

VI. Experimental Results

In this section, the experimental results are presented to validate the effectiveness of our OBA scheme. Specifically, all 16 video sequences from JCT-VC test set [35] are compressed by HEVC with and without RC for comparison. In the experiments, our OBA scheme is compared with the default

[2]It needs to be pointed out that only around 12% CPU is used for encoding a video sequence by HM 14.0 with our OBA scheme, which is far from being fully occupied.

TABLE II
KEY PARAMETERS FOR VIDEO CODING

GOP size	4 frames
CTU size	64×64 pixels
Maximum CTU depth	4
Hierarchical bit allocation	0 or 1
CTU level RC	Enabled

RC scheme of HM 14.0,[3] in which the state-of-the-art R–λ scheme [23] is combined with [28]. In fact, [28] advances the bit allocation of the RC scheme [23] by adopting the weight η_i derived from the R–λ model. Note that the frame/group of pictures (GOP) level bit allocation in our OBA scheme is the same as [28], which is the default setting of HM 14.0.

Details about the parameter setting are presented in Section VI-A. In Section VI-B, we compare the R-D performance of our and R–λ schemes in terms of the objective quality, subjective quality, and Bjontegaard distortion rate (BD rate) for the evaluation of *objective I*. The assessment on bitrate error at CTU, frame, and video levels is introduced in Section VI-C for the evaluation on *objective II*. In addition, we evaluate the robustness of our OBA scheme on compressing videos with dynamic scene changes. The results are provided in Section VI-D. Finally, to verify the effectiveness of our optimal bit reallocation, Section VI-E compares our schemes with and without optimal bit reallocation in terms of R-D performance and RC accuracy.

A. Parameter Setting

In our experiments, all 16 video sequences from classes B, C, D, and E of test set [35] and one additional video sequence with scene changes were chosen for evaluation. All these sequences were encoded with full frames at their default frame rates. Moreover, the way we chose target bitrates was the same as that of [23]. To be more specific, we first encoded each video sequence at fixed QPs, i.e., non-RC encoding for HM 14.0. The fixed QPs were 37, 32, 27, and 22 to ensure enough varying range of quality for compressed videos. Then, the actual bitrates used for compressing the video sequences at four fixed QPs were set as the target bitrates for both our and R–λ schemes. This way, the efficiency of our OBA scheme is evaluated in a more reasonable way with the compressed video sequences ranging from low quality to high quality.

Furthermore, the low-delay IPPP structure, which is the common case in practical applications [23], was chosen for comparison by using the HM default configuration file *encoder_lowdelay_P_main.cfg*. Note that both hierarchical and nonhierarchical encoding were involved in our experiment. Some of the key parameters related to our experiments are listed in Table II. Other parameters were set by default.

B. R-D Assessment

In this section, we concentrate on the assessment of R-D performance for both our OBA and existing R–λ schemes [23], [28] in terms of objective quality, BD rates, and subjective quality.

[3]The latest HM 16.0 adopts the same RC as that of HM 14.0.

TABLE III
Y-PSNR INCREASE OF OUR OBA SCHEME OVER THE R–λ SCHEME [23], [28] FOR ALL 16 VIDEO SEQUENCES

Fixed QP	Non-hierarchical (dB)			Hierarchical (dB)		
	Min.	Max.	Avg.	Min.	Max.	Avg.
37	0.08	0.38	0.27	0.07	0.44	0.21
32	0.12	0.40	0.25	0.05	0.41	0.20
27	0.06	0.43	0.17	0.03	0.31	0.16
22	-0.05	0.20	0.06	-0.05	0.15	0.04
Overall improvement	–	–	0.19	–	–	0.15

For objective quality assessment, we tested all 16 video sequences from JCT-VC test set [35]. Table III presents the overall quality improvement of our OBA scheme over the R–λ scheme in terms of the Y-PSNRs (peak signal to noise ratio) averaged over all 16 test sequences. In this table, the target bitrates were set to be the actual bits obtained by compressing the same sequences at fixed QP values with non-RC HEVC encoding. The QP values are 37, 32, 27, and 22, as reported in the first column of Table III. As can be seen from this table, in comparison with the R–λ scheme, our OBA scheme offers better averaged Y-PSNRs on compressing all 16 sequences at different bitrates for both nonhierarchical and hierarchical encoding. It can be further observed that this improvement can be stably achieved on almost all compressed videos.

Moreover, the overall R-D comparison between our and R–λ schemes is evaluated in terms of BD rate. Table IV reports the averaged BD-rate saving of our OBA scheme over the R–λ scheme for compressing all 16 video sequences at four bitrates. It is worth pointing out that these four bitrates correspond to those of non-RC HM 14.0 with QP values being 37, 32, 27, and 22. From this table, we can see that compared with the R–λ scheme, our OBA scheme is able to save on average 6.0% and 5.2% BD rates in nonhierarchical and hierarchical encoding, respectively. We also tabulate in Table IV the BD-rate saving of our OBA scheme over non-RC HM 14.0. We can see that our scheme suffers about 3.8% BD-rate loss when introducing RC for nonhierarchical HEVC encoding. This is probably because hierarchical QPs are applied to the non-RC encoding, whereas nonhierarchical scenario is set in our OBA scheme with the gain on bit smoothness. However, the gap between RC and non-RC encoding is significantly reduced in our OBA scheme, in comparison with the R–λ scheme. More importantly, for hierarchical encoding, our scheme outperforms both non-RC and R–λ RC schemes. It is worth pointing out that our RC scheme, which enables RC in HEVC, even has a 2.7% BD-rate saving over non-RC HEVC.

In addition, we present details about the R-D curves of four video sequences, which are selected from all 16 video sequences. Similar results can be found for other video sequences. Figs. 4 and 5 show the R-D curves of our OBA, the R–λ [23], [28], and non-RC schemes in both hierarchical and nonhierarchical settings. In these figures, the distortion is evaluated in terms of Y-PSNR. It can be seen that the R-D performance of our OBA scheme is superior to that of the R–λ scheme, especially at low bitrates. For example, when encoding *Fourpeople* with nonhierarchical setting, there is 0.33 dB Y-PSNR increase at 226 197 bps and 0.40 dB

TABLE IV

BD-RATE SAVING OF OUR OBA SCHEMES WITH AND WITHOUT THE OPTIMAL BIT REALLOCATION OVER THE R–λ [23], [28] AND NON-RC SCHEMES ON HM 14.0, AVERAGED OVER ALL 16 VIDEO SEQUENCES

	HM 14.0 with non-RC as an anchor		HM 14.0 with R-λ [23] [28] as an anchor	
	Non-hierarchical	Hierarchical	Non-hierarchical	Hierarchical
OBA	-3.8%	2.7%	6.0%	5.2%
OBA without bit re-allocation	-6.0%	1.5%	3.4%	2.7%

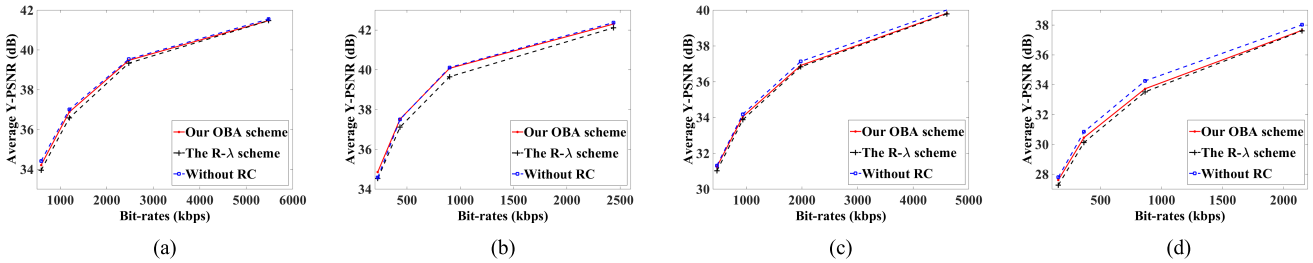

Fig. 4. R-D curve comparison between our OBA, R–λ, and non-RC schemes on compressing four video sequences with nonhierarchial HEVC encoding. (a) *Kimono* (1080p). (b) *Fourpeople* (720p). (c) *BQMall* (480p). (d) *BlowingBubble* (240p).

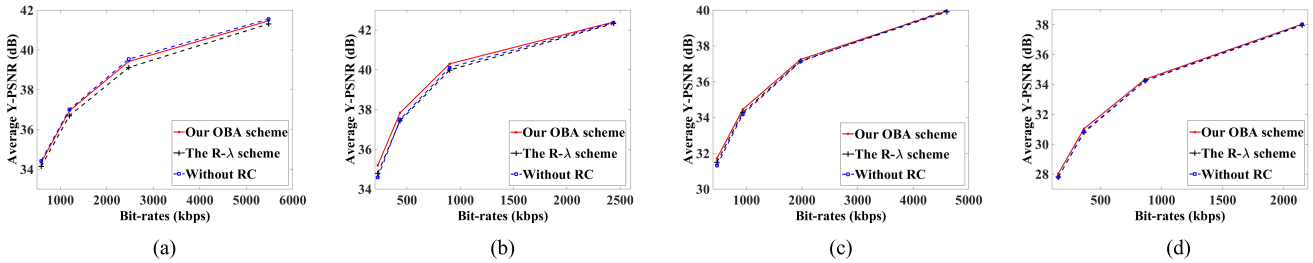

Fig. 5. R-D curve comparison between our OBA, R–λ, and non-RC schemes on compressing four video sequences with hierarchial HEVC encoding. (a) *Kimono* (1080p). (b) *Fourpeople* (720p). (c) *BQMall* (480p). (d) *BlowingBubble* (240p).

improvement at 434 966 bps, whereas only 0.19 dB enhancement of Y-PSNR can be achieved at 2 438 860 bps. This allows our OBA scheme to be more practical in visual communication in which the bandwidth is always limited. Besides, one may observe from Fig. 5 that our OBA scheme has even better R-D results than non-RC when compressing video sequences with hierarchical setting. Again, this implies the potential application of the proposed OBA scheme in the non-RC scenario.

Finally, we move to the assessment on subjective visual quality. We show in Fig. 6 the subjective quality of some video sequences compressed by HM 14.0 with our OBA and the existing R–λ schemes. Obviously, there exists evident visual quality improvement of our OBA scheme over the R–λ scheme.

C. RC Accuracy

Now, we move to the evaluation of the RC accuracy. In this section, the RC accuracy is evaluated at CTU, frame, and the video levels in terms of bitrate error [23] and normalized root mean square error (NRMSE) [30].

1) CTU Level: At CTU level, the RC accuracy of our scheme is evaluated by bitrate error. We here adopt $E_{b,i}$ to evaluate bitrate error of the ith CTU

$$E_{b,i} = \left| \frac{r_i - r_{a,i}}{r_i} \right| \tag{29}$$

which represents the absolute difference between the target and actual bits for each CTU. Recall that in (29) r_i and $r_{a,i}$ stand for the target and actual bits for the ith CTU, respectively. Then, the $E_{b,i}$ averaged over all CTUs of compressed videos at four bitrates is reported in Table V. From this table, we can see that our OBA scheme has much smaller values of $E_{b,i}$ than those of the R–λ scheme for all video sequences. This verifies the superior performance of our scheme on RC accuracy at the CTU level. This is also in accordance with the results of Table I, which validates that our scheme can better estimate R-D relationship to achieve more accurate RC. Note that although the bitrate errors are dramatically reduced in our scheme, such errors are not sufficiently small, especially for the hierarchical scenario. Efforts on further reducing the bitrate errors are an interesting future work.

2) Frame Level: Apart from the bitrate accuracy at CTU level, the bit fluctuation at frame level is another component in evaluating the RC accuracy. To evaluate bit fluctuation, Fig. 7 compares the actual encoding bits per frame or per GOP between our OBA and the state-of-the-art R–λ schemes. Clearly, we can find from this figure that our scheme is far more steady than the R–λ scheme in controlling the encoding bits of HEVC at frame level. Next, we further assess the bit fluctuation via NRMSE from the aspect of the gap between actual and target bits at frame level. It is important to point out that in HEVC, the target bits are always smooth for each frame

(a) (b)

Fig. 6. Subjective quality comparison for our OBA and R–λ [23], [28] schemes. Note that we show the 18th decoded frame of *Fourpeople* compressed at 226 197 bps in nonhierarchical setting and the 13th decoded frame of *Kimono* compressed at 588 306 bps in hierarchical setting. (a) R–λ scheme [23], [28]. (b) Our OBA scheme.

TABLE V

COMPARISON OF RC ACCURACY AT CTU LEVEL BETWEEN THE R–λ [23], [28] AND OUR SCHEMES OVER ALL 16 VIDEO SEQUENCES AT HIERARCHICAL (H) AND NONHIERARCHICAL (NH) SETTINGS

		416 × 240				832 × 480				1080 × 720			1920 × 1080				
		RaceHorse	*BlowingBubbles*	*BasketballPass*	*BQSquare*	*BasketballDrill*	*PartyScene*	*RaceHorseC*	*BQMall*	*Johnny*	*KristenAndSara*	*Fourpeople*	*BasketballDrive*	*Kimono*	*BQTerrace*	*ParkScene*	*Cactus*
NH	[23]	20.34	25.49	42.72	6.73	39.04	72.03	80.56	21.31	4.30	8.68	9.00	44.51	9.76	6.85	30.41	16.23
	Our	1.30	3.18	2.64	1.43	5.26	5.15	4.48	2.41	1.34	1.84	2.40	6.95	5.75	1.56	4.01	4.22
H	[23]	5.02	8.04	11.36	3.14	13.04	38.44	12.39	7.00	3.53	5.11	6.02	15.06	5.62	1.33	10.32	9.89
	Our	0.40	1.31	0.57	1.17	1.22	2.21	0.71	0.78	1.02	0.94	1.26	1.12	1.76	1.33	1.49	1.19

in nonhierarchical encoding and for each GOP in hierarchical encoding. Therefore, the gap between target and actual bits at frame or GOP level can be calculated to reflect the smoothness of bit costs. Here, such a gap can be quantified via NRMSE, which measures the root mean square error between target and actual bits for each frame. In this paper, we follow the method of [30] to calculate NRMSE by

$$\text{NRMSE} = \frac{1}{\bar{R}_{\text{act}}}\sqrt{\frac{\sum_{f=1}^{F_r}(R_{\text{act}}^f - R_{\text{tar}}^f)^2}{F_r}} \tag{30}$$

where F_r denotes the total number of frames, and $\bar{R}_{\text{act}}$ is the actual bits average over all F_r frames. In addition, R_{act}^f and R_{tar}^f stand for the actual and target bits for the fth frame, respectively. Note that a small value of NRMSE indicates slight difference between the actual and target bits for all video frames.

Table VI tabulates the averaged NRMSE results of compressing all 16 test video sequences on HM 14.0 platform with our OBA and the R–λ RC schemes. We can find that our scheme has much lower NRMSE than the R–λ scheme. It clearly reveals that our OBA scheme is capable of making the actually consumed bits closer to the target bits for each frame/GOP.

3) Video Level: At video level, Table VIII presents the bitrate errors of compressing four sequences by HEVC with our and the R–λ RC schemes. Similar results can be found for other video sequences. Generally speaking, in comparison with the R–λ scheme, due to our R-D estimation, our OBA scheme is capable of more precisely controlling encoding

TABLE VI

NRMSE COMPARISON OF OUR OBA AND THE R–λ [23], [28] SCHEMES WHEN COMPRESSING ALL 16 VIDEO SEQUENCES

Fixed QP	Non-hierarchical (%)			Hierarchical (%)		
	OBA	R-λ	Red.	OBA	R-λ	Red.
37	3.195	5.966	2.771	4.494	10.678	6.184
32	3.272	5.862	2.590	5.265	12.966	7.701
27	3.761	6.078	2.317	7.246	12.326	5.080
22	4.801	7.139	2.338	8.318	15.893	7.575
Average	3.757	6.261	2.504	6.331	12.966	6.635

TABLE VII

COMPARISON OF RC ACCURACY AT VIDEO LEVEL OF OUR OBA AND THE R–λ [23], [28] SCHEMES WHEN COMPRESSING ALL 16 VIDEO SEQUENCES

Fixed QP	Non-hierarchical (‰)			Hierarchical (‰)		
	OBA	R-λ	Red.	OBA	R-λ	Red.
37	0.05	0.06	0.01	0.10	0.12	0.02
32	0.04	0.06	0.02	0.09	0.09	0.00
27	0.03	0.16	0.13	0.04	0.31	0.27
22	0.03	0.08	0.05	0.03	0.35	0.32
Average	0.045	0.090	0.045	0.065	0.218	0.153

TABLE VIII
RESULTS OF HEVC ENCODING BITRATE ERROR FOR OUR OBA AND THE R–λ [23], [28] RC SCHEMES

Video sequence	Fixed QP	Target bit-rate	Non-hierarchial					Hierarchial				
			OBA scheme		R-λ scheme		Red.	OBA scheme		R-λ scheme		Red.
			Value	Error	Value	Error		Value	Error	Value	Error	
		(bps)	(bps)	(‰)	(bps)	(‰)	(‰)	(bps)	(‰)	(bps)	(‰)	(‰)
BQTerrace	37	844,260	844,267	0.01	844,276	0.02	0.01	844,279	0.02	844,299	0.05	0.03
	32	2,356,727	2,356,737	0.00	2,356,742	0.01	0.01	2,356,775	0.02	2,356,764	0.02	0.00
	27	9,745,023	9,745,169	0.01	9,745,212	0.02	0.01	9,745,274	0.03	9,745,347	0.03	0.00
	22	64,553,893	64,554,234	0.01	64,554,221	0.01	0.00	64,554,219	0.02	64,554,173	0.01	-0.01
Johnny	37	98,151	98,150	0.01	98,158	0.07	0.06	98,136	0.15	98,155	0.04	-0.11
	32	190,084	190,090	0.03	190,092	0.04	0.01	190,085	0.00	190,086	0.01	0.01
	27	459,634	459,643	0.02	459,645	0.02	0.00	459,636	0.01	459,646	0.03	0.02
	22	1,860,823	1,860,909	0.05	1,860,882	0.03	-0.02	1,860,900	0.04	1,860,914	0.05	0.01
PartyScene	37	658,368	658,370	0.00	658,376	0.01	0.01	658,387	0.03	658,413	0.07	0.04
	32	1,564,746	1,564,800	0.03	1,564,793	0.03	0.00	1,564,738	0.01	1,564,834	0.06	0.05
	27	3,700,951	3,700,974	0.01	3,701,022	0.02	0.01	3,701,058	0.03	3,701,099	0.04	0.01
	22	9,328,842	9,328,890	0.01	9,328,862	0.00	-0.01	9,328,878	0.00	9,328,670	0.02	0.02
BQSquare	37	130,762	130,771	0.06	130,770	0.06	0.00	130,762	0.00	130,779	0.13	0.13
	32	336,838	336,824	0.04	336,864	0.08	0.04	336,875	0.11	336,866	0.08	-0.03
	27	908,753	908,742	0.01	908,778	0.03	0.02	908,796	0.05	908,802	0.05	0.00
	22	2,760,406	2,760,443	0.01	2,760,457	0.02	0.01	2,760,456	0.02	2,760,430	0.01	-0.01

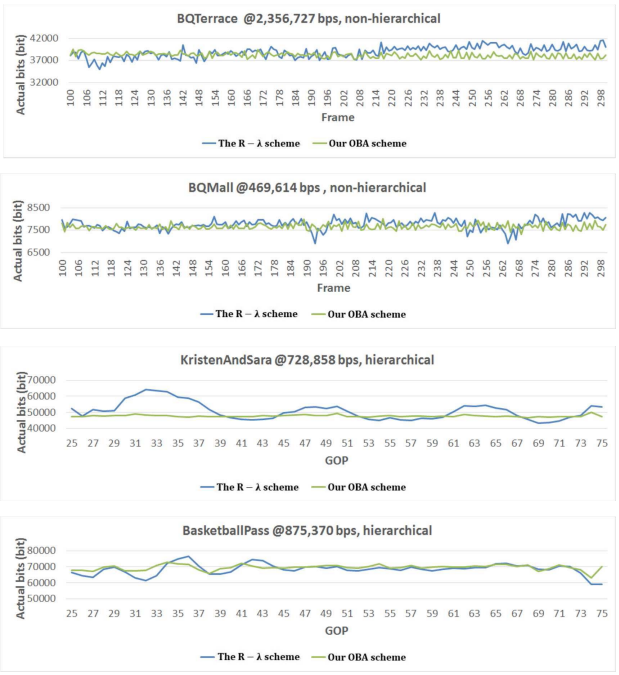

Fig. 7. Bit fluctuation of our OBA and the R–λ schemes [23], [28]. For nonhierarchical encoding, actual bits per frame are shown. For hierarchical encoding, actual bits per GOP are shown. Similar fluctuation results can be found for other encoded video sequences.

bitrates for both nonhierarchical and hierarchical settings. In addition, we tabulate in Table VII the averaged bitrate errors of compressing all 16 sequences. One can see that the averaged bitrate errors in our OBA scheme are dramatically reduced for both nonhierarchical and hierarchical encoding.

D. Robust Test on Scene Change Videos

In this section, one additional video sequence with dynamic scene changes, *Mobisode*, together with *Kimono*, was compressed to evaluate the robustness of the RC schemes. Note that in JCT-VC test set, only *Kimono* has dynamic scheme changes. Since the bit fluctuation and quality deviation of hierarchical setting are larger than those of nonhierarchical setting, Table IX shows the R-D performance of our OBA and the R–λ schemes for the hierarchical encoding. Similar results can be found for the nonhierarchical setting. From this table, we can see that the proposed OBA scheme has 0.20 dB Y-PSNR improvement on average over the existing R–λ scheme. This improvement is even higher than 0.15 dB, which is the averaged improvement over the 16 video sequences in the JCT-VC test set. It implies that our scheme is robust on quality improvement for videos with dynamic scene changes.

In addition, as can be seen from Table IX, the RC error of our scheme is largely reduced, i.e., from 3.9‰ to 0.35‰. We further show in Fig. 8 the maps of bitrate errors from the 139th to 142nd frames of *Kimono*, in which scene change occurs. This figure shows that the bitrate errors of our scheme can be assumed to small values within three frames after the scene change. On the contrary, in the conventional R–λ scheme, the bitrate errors for the next three frames remain at large values. It implies that the straightforward updating on the c_i and k_i of our R-D estimation can adjust to scene change at a faster speed than the gradual updating of the R–λ estimation. Therefore, our scheme is able to quickly adapt to video content when the scene changes, thus being robust to various video sequences.

In summary, our OBA scheme is able to obtain a stable and even better performance on the R-D performance and RC accuracy when compressing the videos with dynamic scene changes.

E. Evaluation of the Proposed Bit Reallocation Method

It is necessary to evaluate the performance of our optimal bit reallocation method, which is adopted in our scheme. Since there exists a difference between the target and actual bitrates when encoding each CTU, the optimal bit reallocation is developed in our scheme to ensure RC accuracy. Here, we report in Table X the averaged bitrate errors of our OBA scheme with and without bit reallocation. From this table, we

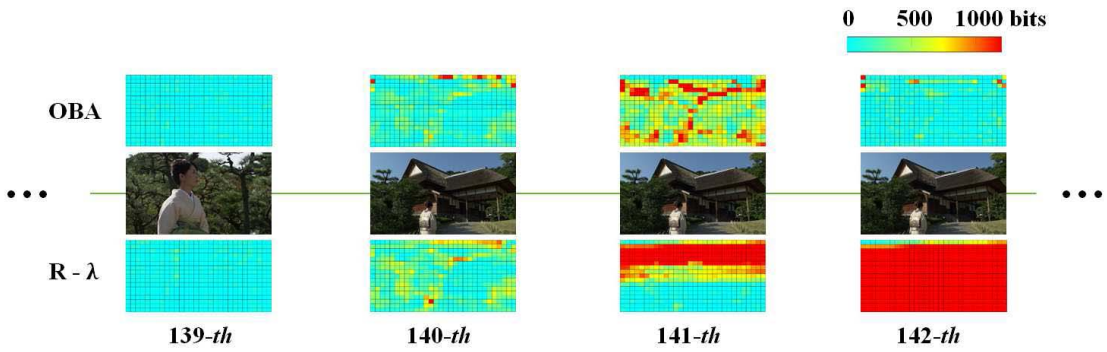

Fig. 8. Maps of bitrate errors of *Kimono* for our OBA and the R–λ schemes at 1 195 000 bps with nonhierarchical setting.

TABLE IX
RESULTS OF HIERARCHICAL ENCODING BETWEEN OUR OBA AND THE R–λ [23], [28] SCHEMES

Sequences	Fixed QP	Target Bit-rates	The R-λ scheme			Our OBA scheme			
		bps	PSNR (dB)	Bit-rates (bps)	Error (‰)	PSNR (dB)	Increment (dB)	Bit-rates (bps)	Error (‰)
Kimono	37	588,306	34.14	588,449	0.24	34.34	0.20	588,447	0.24
	32	1194,990	36.69	1195,124	0.11	36.93	0.24	1195,267	0.23
	27	2472,606	39.12	2472,810	0.08	39.42	0.31	2472,837	0.09
	22	5482,135	41.31	5482,392	0.05	41.46	0.15	5482,524	0.07
Mobisode	37	54,937	38.26	54,970	0.60	38.42	0.16	54,913	0.44
	32	102,434	40.42	103,463	10.05	40.61	0.19	102,402	0.31
	27	214,675	42.46	218,982	20.06	42.59	0.13	214,382	1.36
	22	502,154	43.84	502,150	0.01	44.03	0.19	501,717	0.08
Average PSNR Increment			−−			0.20 dB			
Average $Error$			3.90 ‰			0.35 ‰			

TABLE X
COMPARISON OF BITRATE ERROR OF OUR OBA WITH (OBA) AND WITHOUT BIT REALLOCATION (OBA W/O), AVERAGED OVER ALL 16 VIDEO SEQUENCES

Fixed QP	Non-hierarchical (‰)		Hierarchical (‰)	
	OBA	OBA W/O	OBA	OBA W/O
37	0.05	2.70	0.10	3.71
32	0.04	1.42	0.09	1.88
27	0.03	0.72	0.04	1.28
22	0.03	0.47	0.03	0.83
Average	0.045	1.33	0.065	1.93

can see that the bitrate errors are greatly reduced by our bit reallocation method. For example, when enabling bit reallocation in our OBA scheme, the bitrate errors, averaged over all 16 sequences at four bitrates, decrease from 1.33 to 0.045 for nonhierarchical encoding and from 1.93 to 0.065 for hierarchical encoding, respectively.

Next, we move to compare the R-D performance of our OBA scheme with and without bit reallocation. The last row of Table IV shows the averaged BD-rate saving of our OBA scheme without bit reallocation method. From this table, we can see that our scheme without bit reallocation has a better R-D performance than the R–λ scheme, verifying the effectiveness of the OBA by our RTE method. Once the optimal bit reallocation is enabled, our OBA scheme has more BD-rate saving for both hierarchical and nonhierarchical encoding. In general, Table IV implies that our OBA scheme is able to maintain R-D optimization when introducing the optimal bit reallocation. On the other hand, the RC accuracy is significantly improved by our bit reallocation method.

In summary, our OBA scheme outperforms the state-of-the-art R–λ RC scheme [23], [28] of HEVC in all four aspects: 1) the R-D performance is improved by OBA scheme; 2) our OBA scheme has higher RC accuracy at CTU, frame, and video levels; 3) our OBA scheme is more robust to scene change videos; and 4) the optimal bit reallocation of our OBA scheme helps in improving RC accuracy with optimization of R-D performance.

VII. CONCLUSION

In this paper, we have proposed a new scheme, namely, OBA scheme, to optimally allocate bits for CTU level RC in HEVC. More specifically, we first established a novel R-D estimation to better reflect the R-D relationship for each CTU. This estimation contributes a lot to the OBA as well as RC accuracy. Based on the R-D estimation, a formulation on OBA was developed using Lagrange multiplier in distortion minimization with a bitrate constraint. Unfortunately, it is intractable to develop a closed-form solution to the established formulation. Thus, the RTE method was proposed in our OBA scheme to solve the OBA formulation. In light of the proposed RTE method, both OBA and reallocation were achieved for CTU level RC in HEVC. Moreover, it was demonstrated that the convergence speed of the proposed scheme is extremely fast, according to both theoretical and numerical analyses. This leads to a small computational cost for our OBA scheme. As such, OBA can be achieved in our OBA scheme with little extra time cost. Finally, experimental results verified that our OBA scheme outperforms the state-of-the-art R–λ scheme for RC in HEVC from the aspects of R-D performance, RC accuracy, and robustness on the dynamic scene changes.

APPENDIX A
PROOF OF LEMMA 1

For $a_i > \lambda > 0$, $\tilde{\lambda} > \lambda > 0$, and $b_i > 0$, we can acquire $((\ln a_i/\lambda)^n/n!)b_i^n > 0$ and $\tilde{r}_i\ ((\ln\tilde{\lambda}/\lambda)^n/n!)b_i^n > 0$. Besides, $|n + 1/\ln(\tilde{\lambda}/\lambda)b_i| > |n + 1/\ln(a_i/\lambda)b_i|$ can be rewritten as $(n + 1/\ln(\tilde{\lambda}/\lambda)b_i) > (n + 1/\ln(a_i/\lambda)b_i) > 0$. Then, according to Taylor expansion for $(a_i/\lambda)^{b_i} = \tilde{r}_i(\tilde{\lambda}/\lambda)^{b_i}$, the proof of (22) is equivalent to proving

$$\left(\frac{a_i}{\lambda}\right)^{b_i} - 1 - \frac{\ln\left(\frac{a_i}{\lambda}\right)}{1!}b_i - \frac{\left(\ln\frac{a_i}{\lambda}\right)^2}{2!}b_i^2 - \cdots - \frac{\left(\ln\frac{a_i}{\lambda}\right)^N}{N!}b_i^N > \tilde{r}_i\left(\frac{\tilde{\lambda}}{\lambda}\right)^{b_i} - \tilde{r}_i - \tilde{r}_i\frac{\ln\left(\frac{\tilde{\lambda}}{\lambda}\right)}{1!}b_i - \tilde{r}_i\frac{\left(\ln\frac{\tilde{\lambda}}{\lambda}\right)^2}{2!}b_i^2 - \cdots - \tilde{r}_i\frac{\left(\ln\frac{\tilde{\lambda}}{\lambda}\right)^N}{N!}b_i^N. \tag{31}$$

For the Nth term, the proof can be accomplished in the following two cases.

Case 1:

$$\frac{\left(\ln\frac{a_i}{\lambda}\right)^N}{N!}b_i^N \le \tilde{r}_i\frac{\left(\ln\frac{\tilde{\lambda}}{\lambda}\right)^N}{N!}b_i^N. \tag{32}$$

Since $(n + 1/\ln(\tilde{\lambda}/\lambda)b_i) > (n + 1/\ln(a_i/\lambda)b_i) > 0$, the following holds in this case for $n = 0, 1, 2, 3, \ldots, N-1$:

$$\begin{aligned}\frac{\left(\ln\frac{a_i}{\lambda}\right)^n}{n!}b_i^n &= \frac{\left(\ln\frac{a_i}{\lambda}\right)^N}{N!}b_i^N \cdot \frac{N}{\ln\frac{a_i}{\lambda}b_i} \cdot \frac{N-1}{\ln\frac{a_i}{\lambda}b_i} \cdot \cdots \cdot \frac{n+1}{\ln\frac{a_i}{\lambda}b_i} \\ &< \tilde{r}_i\frac{\left(\ln\frac{\tilde{\lambda}}{\lambda}\right)^N}{N!}b_i^N \cdot \frac{N}{\ln\frac{\tilde{\lambda}}{\lambda}b_i} \cdot \frac{N-1}{\ln\frac{\tilde{\lambda}}{\lambda}b_i} \cdot \cdots \cdot \frac{n+1}{\ln\frac{\tilde{\lambda}}{\lambda}b_i} \\ &= \tilde{r}_i\frac{\left(\ln\frac{\tilde{\lambda}}{\lambda}\right)^n}{n!}b_i^n. \end{aligned} \tag{33}$$

Therefore, we have

$$\begin{aligned}&\left(\frac{a_i}{\lambda}\right)^{b_i} - 1 - \frac{\ln\left(\frac{a_i}{\lambda}\right)}{1!}b_i - \frac{\left(\ln\frac{a_i}{\lambda}\right)^2}{2!}b_i^2 - \cdots - \frac{\left(\ln\frac{a_i}{\lambda}\right)^N}{N!}b_i^N \\ &> \left(\frac{a_i}{\lambda}\right)^{b_i} - \tilde{r}_i - \tilde{r}_i\frac{\ln\left(\frac{\tilde{\lambda}}{\lambda}\right)}{1!}b_i - \tilde{r}_i\frac{\left(\ln\frac{\tilde{\lambda}}{\lambda}\right)^2}{2!}b_i^2 - \cdots - \tilde{r}_i\frac{\left(\ln\frac{\tilde{\lambda}}{\lambda}\right)^N}{N!}b_i^N \\ &= \tilde{r}_i\left(\frac{\tilde{\lambda}}{\lambda}\right)^{b_i} - \tilde{r}_i - \tilde{r}_i\frac{\ln\left(\frac{\tilde{\lambda}}{\lambda}\right)}{1!}b_i - \tilde{r}_i\frac{\left(\ln\frac{\tilde{\lambda}}{\lambda}\right)^2}{2!}b_i^2 - \cdots - \tilde{r}_i\frac{\left(\ln\frac{\tilde{\lambda}}{\lambda}\right)^N}{N!}b_i^N. \end{aligned} \tag{34}$$

Case 2:

$$\frac{\left(\ln\frac{a_i}{\lambda}\right)^N}{N!}b_i^N > \tilde{r}_i\frac{\left(\ln\frac{\tilde{\lambda}}{\lambda}\right)^N}{N!}b_i^N. \tag{35}$$

Since $(n + 1/\ln(\tilde{\lambda}/\lambda)b_i) > (n + 1/\ln(a_i/\lambda)b_i) > 0$, the following holds in this case for $n = N+1, N+2, N+3, \ldots$:

$$\begin{aligned}\frac{\left(\ln\frac{a_i}{\lambda}\right)^n}{n!}b_i^n &= \frac{\left(\ln\frac{a_i}{\lambda}\right)^N}{N!}b_i^N \cdot \frac{\ln\frac{a_i}{\lambda}b_i}{N+1} \cdot \frac{\ln\frac{a_i}{\lambda}b_i}{N+2} \cdot \cdots \cdot \frac{\ln\frac{a_i}{\lambda}b_i}{n+1} \\ &> \tilde{r}_i\frac{\left(\ln\frac{\tilde{\lambda}}{\lambda}\right)^N}{N!}b_i^N \cdot \frac{\ln\frac{\tilde{\lambda}}{\lambda}b_i}{N+1} \cdot \frac{\ln\frac{\tilde{\lambda}}{\lambda}b_i}{N+2} \cdot \cdots \cdot \frac{\ln\frac{a_i}{\lambda}b_i}{n+1} = \tilde{r}_i\frac{\left(\ln\frac{\tilde{\lambda}}{\lambda}\right)^n}{n!}b_i^n. \end{aligned} \tag{36}$$

Thus, the inequality below can be obtained

$$\begin{aligned}&\left(\frac{a_i}{\lambda}\right)^{b_i} - 1 - \frac{\ln\left(\frac{a_i}{\lambda}\right)}{1!}b_i - \frac{\left(\ln\frac{a_i}{\lambda}\right)^2}{2!}b_i^2 - \cdots - \frac{\left(\ln\frac{a_i}{\lambda}\right)^N}{N!}b_i^N \\ &= \frac{\left(\ln\frac{a_i}{\lambda}\right)^{N+1}}{N+1!}b_i^{N+1} + \frac{\left(\ln\frac{a_i}{\lambda}\right)^{N+2}}{N+2!}b_i^{N+2} + \frac{\left(\ln\frac{a_i}{\lambda}\right)^{N+3}}{N+3!}b_i^{N+3} + \cdots \\ &> \tilde{r}_i\frac{\left(\ln\frac{\tilde{\lambda}}{\lambda}\right)^{N+1}}{N+1!}b_i^{N+1} + \tilde{r}_i\frac{\left(\ln\frac{\tilde{\lambda}}{\lambda}\right)^{N+2}}{N+2!}b_i^{N+2} + \tilde{r}_i\frac{\left(\ln\frac{\tilde{\lambda}}{\lambda}\right)^{N+3}}{N+3!}b_i^{N+3} + \cdots \\ &= \tilde{r}_i\left(\frac{\tilde{\lambda}}{\lambda}\right)^{b_i} - \tilde{r}_i - \tilde{r}_i\frac{\ln\left(\frac{\tilde{\lambda}}{\lambda}\right)}{1!}b_i - \tilde{r}_i\frac{\left(\ln\frac{\tilde{\lambda}}{\lambda}\right)^2}{2!}b_i^2 - \cdots - \tilde{r}_i\frac{\left(\ln\frac{\tilde{\lambda}}{\lambda}\right)^N}{N!}b_i^N. \end{aligned} \tag{37}$$

Therefore, taking into account the above two cases, the following inequality exists:

$$\left(\frac{a_i}{\lambda}\right)^{b_i} - 1 - \frac{\ln\left(\frac{a_i}{\lambda}\right)}{1!}b_i - \frac{\left(\ln\frac{a_i}{\lambda}\right)^2}{2!}b_i^2 - \cdots - \frac{\left(\ln\frac{a_i}{\lambda}\right)^N}{N!}b_i^N > \tilde{r}_i\left(\frac{\tilde{\lambda}}{\lambda}\right)^{b_i} - \tilde{r}_i - \tilde{r}_i\frac{\ln\left(\frac{\tilde{\lambda}}{\lambda}\right)}{1!}b_i - \tilde{r}_i\frac{\left(\ln\frac{\tilde{\lambda}}{\lambda}\right)^2}{2!}b_i^2 - \cdots - \tilde{r}_i\frac{\left(\ln\frac{\tilde{\lambda}}{\lambda}\right)^N}{N!}b_i^N. \tag{38}$$

This completes the proof of Lemma 1.

APPENDIX B
PROOF OF PROPOSITION 2

Toward the Taylor expansion of $\sum_{i=1}^{M}\tilde{r}_i(\tilde{\lambda}/\lambda)^{b_i}$ in (23), we have the following equations:

$$\begin{aligned}R &= \sum_{i=1}^{M}\tilde{r}_i\left(\frac{\tilde{\lambda}}{\lambda}\right)^{b_i} \\ &= \sum_{i=1}^{M}\tilde{r}_i + \sum_{i=1}^{M}\tilde{r}_i\frac{\ln\left(\frac{\tilde{\lambda}}{\lambda}\right)}{1!}b_i + \sum_{i=1}^{M}\tilde{r}_i\frac{\left(\ln\frac{\tilde{\lambda}}{\lambda}\right)^2}{2!}b_i^2 + \sum_{i=1}^{M}\tilde{r}_i\frac{\left(\ln\frac{\tilde{\lambda}}{\lambda}\right)^3}{3!}b_i^3 \\ &= \sum_{i=1}^{M}\tilde{r}_i + \sum_{i=1}^{M}\tilde{r}_i\frac{\ln\left(\frac{\tilde{\lambda}}{\lambda}\right)}{1!}b_i + \sum_{i=1}^{M}\tilde{r}_i\frac{\left(\ln\frac{\tilde{\lambda}}{\lambda}\right)^2}{2!}b_i^2 \\ &\quad + \sum_{i=1}^{M}\tilde{r}_i\frac{\left(\ln\frac{\tilde{\lambda}}{\lambda}\right)^3}{3!}b_i^3 + \sum_{i=1}^{M}\tilde{r}_i\frac{\left(\ln\frac{\tilde{\lambda}}{\lambda}\right)^4}{4!}b_i^4 \\ &\quad + \sum_{i=1}^{M}\tilde{r}_i\frac{\left(\ln\frac{\tilde{\lambda}}{\lambda}\right)^5}{5!}b_i^5 + \cdots \end{aligned} \tag{39}$$

For $\tilde{\lambda} > \lambda > 0$ and $b_i > 0$, we can obtain $(\ln(\tilde{\lambda}/\lambda)) \cdot b_i > 0$. Moreover, as $(\tilde{\lambda}/\lambda) > 1$, there exists $R > \sum_{i=1}^{M}\tilde{r}_i > 0$. Thus, with $(\ln(\tilde{\lambda}/\lambda)) \cdot b_i > 0$ and $R > \sum_{i=1}^{M}\tilde{r}_i > 0$ in (39), $\ln(\tilde{\lambda}/\hat{\lambda}) > \ln(\tilde{\lambda}/\lambda) > 0$ exists, such that $\hat{\lambda} < \lambda$ can be achieved.

For $\lambda > \tilde{\lambda} > 0$ and $b_i > 0$, we have

$$\sum_{i=1}^{M}\tilde{r}_i\frac{\left(\ln\frac{\tilde{\lambda}}{\lambda}\right)^4}{4!}b_i^4 + \sum_{i=1}^{M}\tilde{r}_i\frac{\left(\ln\frac{\tilde{\lambda}}{\lambda}\right)^5}{5!}b_i^5 + \cdots > 0. \tag{40}$$

Then, with (39), the following inequality exists:

$$\sum_{i=1}^{M}\tilde{r}_i\frac{\ln\left(\frac{\tilde{\lambda}}{\hat{\lambda}}\right)}{1!}b_i+\sum_{i=1}^{M}\tilde{r}_i\frac{\left(\ln\frac{\tilde{\lambda}}{\hat{\lambda}}\right)^2}{2!}b_i^2+\sum_{i=1}^{M}\tilde{r}_i\frac{\left(\ln\frac{\tilde{\lambda}}{\hat{\lambda}}\right)^3}{3!}b_i^3 > \sum_{i=1}^{M}\tilde{r}_i\frac{\ln\left(\frac{\tilde{\lambda}}{\lambda}\right)}{1!}b_i+\sum_{i=1}^{M}\tilde{r}_i\frac{\left(\ln\frac{\tilde{\lambda}}{\lambda}\right)^2}{2!}b_i^2+\sum_{i=1}^{M}\tilde{r}_i\frac{\left(\ln\frac{\tilde{\lambda}}{\lambda}\right)^3}{3!}b_i^3. \quad (41)$$

Moreover, seeing $\hat{\lambda}$ and λ as variable x, the inequality (41) can be analyzed by

$$\sum_{i=1}^{M}\tilde{r}_i+\sum_{i=1}^{M}\tilde{r}_i\frac{\ln\left(\frac{\tilde{\lambda}}{x}\right)}{1!}b_i+\sum_{i=1}^{M}\tilde{r}_i\frac{\left(\ln\frac{\tilde{\lambda}}{x}\right)^2}{2!}b_i^2+\sum_{i=1}^{M}\tilde{r}_i\frac{\left(\ln\frac{\tilde{\lambda}}{x}\right)^3}{3!}b_i^3. \quad (42)$$

The function of (42) monotonously decreases to 0 along with the increasing variable x (until $x \le \tilde{\lambda}$). Therefore, we can obtain that $\hat{\lambda} < \lambda$ by combining (41) and (42).

This completes the proof of Proposition 2.

Appendix C
Proof of Lemma 3

Since $\hat{\lambda}$ is the solution of λ to the third-order Taylor expansion of $\sum_{i=1}^{M}\tilde{r}_i(\tilde{\lambda}/\lambda)^{b_i}$, the following equation exists:

$$R=\sum_{i=1}^{M}\tilde{r}_i\left(\frac{\tilde{\lambda}}{\lambda}\right)^{b_i} =\sum_{i=1}^{M}\tilde{r}_i+\sum_{i=1}^{M}\tilde{r}_i\frac{\ln\left(\frac{\tilde{\lambda}}{\hat{\lambda}}\right)}{1!}b_i+\sum_{i=1}^{M}\tilde{r}_i\frac{\left(\ln\frac{\tilde{\lambda}}{\hat{\lambda}}\right)^2}{2!}b_i^2+\sum_{i=1}^{M}\tilde{r}_i\frac{\left(\ln\frac{\tilde{\lambda}}{\hat{\lambda}}\right)^3}{3!}b_i^3. \quad (43)$$

In fact, $0<(\tilde{\lambda}/\lambda)^{b_i}<1$ holds for $0<\tilde{\lambda}<\lambda$ and $b_i>0$. Besides, there exists $R=\sum_{i=1}^{M}\tilde{r}_i(\tilde{\lambda}/\lambda)^{b_i}$ in (43). Therefore, $\sum_{i=1}^{M}\tilde{r}_i > R$ can be obtained.

Next, assuming that $\hat{\lambda}\le\tilde{\lambda}$, we have $\ln(\tilde{\lambda}/\hat{\lambda})\ge 0$. Due to $\sum_{i=1}^{M}\tilde{r}_i > R$, $\ln(\tilde{\lambda}/\hat{\lambda})\ge 0$, and $b_i>0$, the following inequality holds:

$$\sum_{i=1}^{M}\tilde{r}_i+\sum_{i=1}^{M}\tilde{r}_i\frac{\ln\left(\frac{\tilde{\lambda}}{\hat{\lambda}}\right)}{1!}b_i+\sum_{i=1}^{M}\tilde{r}_i\frac{\left(\ln\frac{\tilde{\lambda}}{\hat{\lambda}}\right)^2}{2!}b_i^2+\sum_{i=1}^{M}\tilde{r}_i\frac{\left(\ln\frac{\tilde{\lambda}}{\hat{\lambda}}\right)^3}{3!}b_i^3 > R \quad (44)$$

which is contradictory to (43). Therefore, it can be proved that $\tilde{\lambda}<\hat{\lambda}$. Then, combining with Proposition 1, $\tilde{\lambda}<\hat{\lambda}<\lambda$ can be worked out. As a result, $|\hat{\lambda}-\lambda|<|\tilde{\lambda}-\lambda|$ exists.

This completes the proof of Lemma 3.

Appendix D
Proof of Lemma 4

Since $\tilde{r}_i=(a_i/\tilde{\lambda})^{b_i}$ and $r_i=(a_i/\lambda)^{b_i}$, we can obtain $\tilde{r}_i=r_i\cdot(\lambda/\tilde{\lambda})^{b_i}$. Then, the following Taylor expansion for $\sum_{i=1}^{M}\tilde{r}_i(\tilde{\lambda}/\lambda)^{b_i}=R$ holds for (20) by discarding its fourth and higher order terms:

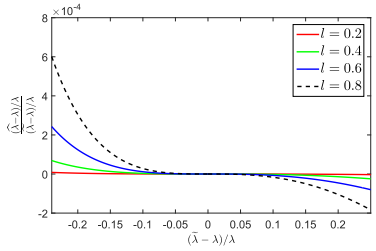

Fig. 9. Relationship between $((\hat{\lambda}-\lambda)/\lambda/(\tilde{\lambda}-\lambda)/\lambda)$ and $(\hat{\lambda}-\lambda/\lambda)$.

$$R=\sum_{i=1}^{M}\tilde{r}_i\left(\frac{\tilde{\lambda}}{\lambda}\right)^{b_i}\approx\sum_{i=1}^{M}\tilde{r}_i+\sum_{i=1}^{M}\tilde{r}_i\frac{\ln\left(\frac{\tilde{\lambda}}{\hat{\lambda}}\right)}{1!}b_i+\sum_{i=1}^{M}\tilde{r}_i\frac{\left(\ln\frac{\tilde{\lambda}}{\hat{\lambda}}\right)^2}{2!}b_i^2+\sum_{i=1}^{M}\tilde{r}_i\frac{\left(\ln\frac{\tilde{\lambda}}{\hat{\lambda}}\right)^3}{3!}b_i^3. \quad (45)$$

Since $\forall i$, $b_i=l\in(0,1)$ and $\sum_{i=1}^{M}r_i=R$, there exists $\sum_{i=1}^{M}\tilde{r}_i=\sum_{i=1}^{M}r_i\cdot(\lambda/\tilde{\lambda})^{b_i}=R\cdot(\lambda/\tilde{\lambda})^{l}$.

Next, we rewrite (45) as

$$\left(\frac{\lambda}{\tilde{\lambda}}\right)^{l}\frac{R\cdot l^3}{3!}\cdot\left(\ln\frac{\tilde{\lambda}}{\hat{\lambda}}\right)^3+\left(\frac{\lambda}{\tilde{\lambda}}\right)^{l}\frac{R\cdot l^2}{2!}\cdot\left(\ln\frac{\tilde{\lambda}}{\hat{\lambda}}\right)^2+\left(\frac{\lambda}{\tilde{\lambda}}\right)^{l}\frac{R\cdot l}{1!}\cdot\ln\frac{\tilde{\lambda}}{\hat{\lambda}}+R\cdot\left(\frac{\lambda}{\tilde{\lambda}}\right)^{l}=R. \quad (46)$$

Solving the above cubic equation, we obtain

$$\hat{\lambda}=\tilde{\lambda}\cdot e^{\frac{1+2(\sqrt[3]{Y_1}+\sqrt[3]{Y_2})}{l}} \quad (47)$$

where

$$Y_1,Y_2=-\frac{1}{8}+\frac{1}{8}\cdot\left(-3\left(\frac{\tilde{\lambda}}{\lambda}\right)^{l}+2\pm\sqrt{9\left(\frac{\tilde{\lambda}}{\lambda}\right)^{2l}-6\left(\frac{\tilde{\lambda}}{\lambda}\right)^{l}+2}\right). \quad (48)$$

With (47), the relationship between $(\tilde{\lambda}-\lambda/\lambda)$ and $(\hat{\lambda}-\lambda/\lambda)$ is plotted in Fig. 9. From this figure, it can be observed that for each iteration, the reduction of $|((\hat{\lambda}-\lambda)/\lambda/(\tilde{\lambda}-\lambda)/\lambda)|$ is able to reach the magnitude of 10^{-3}.

This completes the proof of Lemma 4.

References

[1] S. Li, M. Xu, and Z. Wang, "A novel method on optimal bit allocation at LCU level for rate control in HEVC," in *Proc. IEEE ICME*, Jun./Jul. 2015, pp. 1–6.

[2] T. Wiegand, G. J. Sullivan, G. Bjøntegaard, and A. Luthra, "Overview of the H.264/AVC video coding standard," *IEEE Trans. Circuits Syst. Video Technol.*, vol. 13, no. 7, pp. 560–576, Jul. 2003.

[3] ITU-T VCEG, *Joint Call for Proposals on Video Compression Technology*, document ITU-T VCEG-AM91, and ISO/IEC MPE N11113, Kyoto, Japan, Jan. 2010.

[4] J. R. Ohm and G. J. Sullivan, "High Efficiency Video Coding: The next frontier in video compression [Standards in a Nutshell]," *IEEE Signal Process. Mag.*, vol. 30, no. 1, pp. 152–158, Jan. 2013.

[5] G. J. Sullivan, J.-R. Ohm, W.-J. Han, and T. Wiegand, "Overview of the High Efficiency Video Coding (HEVC) standard," *IEEE Trans. Circuits Syst. Video Technol.*, vol. 22, no. 12, pp. 1649–1668, Dec. 2012.
[6] G. J. Sullivan and J.-R. Ohm, "Recent developments in standardization of High Efficiency Video Coding (HEVC)," *Proc. 33rd SPIE Appl. Dig. Image Process*, vol. 7798, p. 77980V, Sep. 2010.
[7] B. G. Haskell, *Digital Video: An Introduction to MPEG-2*. New York, NY, USA: Springer, 1997.
[8] A. Vetro, H. Sun, and Y. Wang, "MPEG-4 rate control for multiple video objects," *IEEE Trans. Circuits Syst. Video Technol.*, vol. 9, no. 1, pp. 186–199, Feb. 1999.
[9] G. J. Sullivan, T. Wiegand, and K.-P. Lim, "Text description of joint model reference encoding methods and decoding concealment methods, JVT-N046, Jan. 2005.
[10] T. Chiang and Y.-Q. Zhang, "A new rate control scheme using quadratic rate distortion model," *IEEE Trans. Circuits Syst. Video Technol.*, vol. 7, no. 1, pp. 246–250, Feb. 1997.
[11] S. Ma, W. Gao, and Y. Lu, "Rate-distortion analysis for H.264/AVC video coding and its application to rate control," *IEEE Trans. Circuits Syst. Video Technol.*, vol. 15, no. 12, pp. 1533–1544, Dec. 2005.
[12] D.-K. Kwon, M.-Y. Shen, and C.-C. J. Kuo, "Rate control for H.264 video with enhanced rate and distortion models," *IEEE Trans. Circuits Syst. Video Technol.*, vol. 17, no. 5, pp. 517–529, May 2007.
[13] Y. Liu, Z. G. Li, and Y. C. Soh, "A novel rate control scheme for low delay video communication of H.264/AVC standard," *IEEE Trans. Circuits Syst. Video Technol.*, vol. 17, no. 1, pp. 68–78, Jan. 2007.
[14] S. Hu, H. Wang, S. Kwong, T. Zhao, and C.-C. J. Kuo, "Rate control optimization for temporal-layer scalable video coding," *IEEE Trans. Circuits Syst. Video Technol.*, vol. 21, no. 8, pp. 1152–1162, Aug. 2011.
[15] S. Hu, H. Wang, and S. Kwong, "Adaptive quantization-parameter clip scheme for smooth quality in H.264/AVC," *IEEE Trans. Image Process.*, vol. 21, no. 4, pp. 1911–1919, Apr. 2012.
[16] Y. H. Tan, C. Yeo, and Z. Li, "Single-pass rate control with texture and non-texture rate-distortion models," *IEEE Trans. Circuits Syst. Video Technol.*, vol. 22, no. 8, pp. 1236–1245, Aug. 2012.
[17] A. Ortega and K. Ramchandran, "Rate-distortion methods for image and video compression," *IEEE Signal Process. Mag.*, vol. 15, no. 6, pp. 23–50, Nov. 1998.
[18] Z. He, Y. K. Kim, and S. Mitra, "Low-delay rate control for DCT video coding via ρ-domain source modeling," *IEEE Trans. Circuits Syst. Video Technol.*, vol. 11, no. 8, pp. 928–940, Aug. 2002.
[19] M. Liu, Y. Guo, H. Li, and C. W. Chen, "Low-complexity rate control based on ρ-domain model for scalable video coding," in *Proc. IEEE ICIP*, Sep. 2010, pp. 1277–1280.
[20] H. Choi, J. Yoo, J. Nam, D. Sim, and I. V. Bajić, "Pixel-wise unified rate-quantization model for multi-level rate control," *IEEE J. Sel. Topics Signal Process.*, vol. 7, no. 6, pp. 1112–1123, Dec. 2013.
[21] J. Si, S. Ma, and W. Gao, "Efficient bit allocation and CTU level rate control for High Efficiency Video Coding," in *Proc. PCS*, Dec. 2013, pp. 89–92.
[22] S. Wang, S. Ma, S. Wang, D. Zhao, and W. Gao, "Quadratic ρ-domain based rate control algorithm for HEVC," in *Proc. IEEE ICASSP*, May 2013, pp. 1695–1699.
[23] B. Li, H. Li, L. Li, and J. Zhang, "λ domain rate control algorithm for High Efficiency Video Coding," *IEEE Trans. Image Process.*, vol. 23, no. 9, pp. 3841–3854, Sep. 2014.
[24] G. J. Sullivan and T. Wiegand, "Rate-distortion optimization for video compression," *IEEE Signal Process. Mag.*, vol. 15, no. 6, pp. 74–90, Nov. 1998.
[25] S. Wang, S. Ma, S. Wang, D. Zhao, and W. Gao, "Rate-GOP based rate control for High Efficiency Video Coding," *IEEE J. Sel. Topics Signal Process.*, vol. 7, no. 6, pp. 1101–1111, Dec. 2013.
[26] J. Si, S. Ma, S. Wang, and W. Gao, "Laplace distribution based CTU level rate control for HEVC," in *Proc. VCIP*, 2013, pp. 1–6.
[27] H. Sun, S. Gao, and C. Zhang, "Adaptive bit allocation scheme for rate control in High Efficiency Video Coding with initial quantization parameter determination," *Signal Process., Image Commun.*, vol. 29, no. 10, pp. 1029–1045, 2014.
[28] B. Li, H. Li, and L. Li, *Adaptive Bit Allocation for R-Lambda Model Rate Control in HM* document JCTVC-M0036, Apr. 2013.
[29] L. Deng, F. Pu, S. Hu, and C.-C. J. Kuo, "HEVC encoder optimization based on a new RD model and pre-enoding," in *Proc. PCS*, 2014, pp. 1–4.
[30] M. Wang, K. N. Ngan, and H. Li, "An efficient frame-content based intra frame rate control for High Efficiency Video Coding," *IEEE Signal Process. Lett.*, vol. 22, no. 7, pp. 896–900, Jul. 2015.
[31] S. Li, M. Xu, X. Deng, and Z. Wang, "Weight-based R-λ rate control for perceptual HEVC coding on conversational videos," *Signal Process., Image Commun.*, vol. 38, pp. 127–140, Oct. 2015.
[32] M. Dai, D. Loguinov, and H. Radha, "Rate-distortion modeling of scalable video coders," in *Proc. IEEE ICIP*, vol. 2. Oct. 2004, pp. 1093–1096.
[33] S. Mallat and F. Falzon, "Analysis of low bit rate image transform coding," *IEEE Trans. Signal Process.*, vol. 46, no. 4, pp. 1027–1042, Apr. 1998.
[34] T. Wiegand and B. Girod, "Lagrange multiplier selection in hybrid video coder control," in *Proc. IEEE ICIP*, vol. 3. Oct. 2001, pp. 542–545.
[35] F. Bossen, *Common Test Conditions and Software Reference Configurations*, document JCTVC-G1200, Nov. 2011.
[36] S. Fan, "A new extracting formula and a new distinguishing means on the one variable cubic equation," *Natural Sci. J. Hhainan Teach. College*, vol. 2, no. 2, pp. 91–98, Dec. 1989.

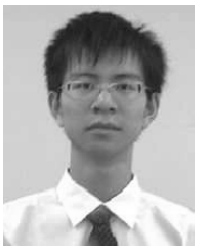

Shengxi Li (M'14) received the bachelor's degree from Beihang University, Beijing, China, in 2014, where he is currently pursuing the master's degree in 2016.

His current research interests include rate distortion theory and perceptual video coding.

Mr. Li was the recipient of Beihang Gold Medal in 2013, which is the highest award for undergraduates in Beihang University, and also was the recipient of Top 10 Postgraduates Award in 2016, which is the highest award for postgraduates in Beihang University

Mai Xu (M'10) received the B.S. degree from Beihang University, Beijing, China, in 2003, the M.S. degree from Tsinghua University, Beijing, in 2006, and the Ph.D. degree from Imperial College London, London, U.K., in 2010.

He was a Research Fellow with the Electrical Engineering Department, Tsinghua University, from 2010 to 2012. Since 2013, he has been with Beihang University as an Associate Professor. He has authored over 50 technical papers in international journals and conference proceedings. His current research interests include visual communication and image processing.

Zulin Wang (M'14) received the B.S. and M.S. degrees in electronics engineering and the Ph.D. degree from Beihang University, Beijing, China, in 1986, 1989, and 2000, respectively.

He is currently the Dean of the School of Electronic and Information Engineering with Beihang University. He has authored or co-authored over 100 papers and holds six patents, and published two books in his research fields. He has undertaken approximately 30 projects related to image/video coding and wireless communication. His current research interests include image processing, electromagnetic countermeasure, and satellite communication technology.

Xiaoyan Sun (M'04–SM'10) received the B.S., M.S., and Ph.D. degrees from the Harbin Institute of Technology, Harbin, China, in 1997, 1999, and 2003, respectively, all in computer science.

She has been with Microsoft Research Asia, Beijing, China, since 2004, where she is currently a Lead Researcher with the Internet Media Group. She has authored or co-authored over 60 journal and conference papers and ten proposals to standards. Her current research interests include image and video compression, image processing, computer vision, and cloud computing.

Dr. Sun was a recipient of the best paper award of the IEEE TRANSACTIONS ON CIRCUITS AND SYSTEMS FOR VIDEO TECHNOLOGY in 2009.